3 CHAPTER
Auto-inhibition and Auto-intervention in One-state Models

Several separate issues relate to biological self-regulation. In the field of ligand–receptor interactions, auto-regulation may relate to either ligand-induced alterations of a receptive unit or to control induced within receptive units *per se*, before further down-stream regulations through feedback.

The themes of this chapter are divided into four divisions. The first division comprises of formulations for the modeling of ligand-dependent auto-inhibition (sub-chapters 3.1–3.3), as well as for a so-called 'low-dose hook-effect' (sub-chapter 3.4); all related to simple auto-intervention in one-state models.

The second division is a general introduction to biological auto-regulation and control (sub-chapter 3.5) which includes reflections on the meaning of 'self'.

The third division deals with concentration-dependent auto-inhibition and time-dependent phenomena, such as ligand-induced desensitization, both types eliciting auto-regulatory inhibition in receptive systems with only one type of ligand present (sub-chapter 3.6). Sub-chapter 3.6 also treats various aspects of desensitization including homologous and heterologous desensitization with actual examples of *intrinsic* (receptor-dependent) and *extrinsic* (phosphorylation-dependent) desensitization.

The fourth division includes additional examples of models related to ligand-dependent auto-inhibition and desensitization (sub-chapter 3.7).

3.1. Auto-intervention. Its Start and Terminology

The formulation of auto-intervention has its own history, it requires certain conditions, and uses a special terminology. Therefore, before formulation of auto-intervention in sub-chapter 3.2, I will recount some conditions and give examples of terms related to auto-intervention.

3.1.1. The Start of Formulating Ligand-dependent Auto-inhibition

Enzymatic substrate-inhibition was originally formulated in 1930 by Sir John Burdon Sanderson Haldane in his treatise 'Enzymes' (Haldane 1930) (see Section 3.2.2).

Long before scientists from other fields, including physiology, enzymologists were formulating a self-induced inhibition by activating ligands, i.e., substrates. Evidently, inhibition can take place for enzymes at high substrate – 'agonist' – concentrations, even when feed-back inhibition due to product generation is ruled out (Kaiser 1980; Kuhl 1994). Thus, no regulatory mechanism can explain the concentration-dependent attenuation of enzymatic activity at high substrate concentration – 'substrate inhibition' – other than through the substrate itself at a likely regulatory site. The result is bell-shaped dose-response curves. Similarly, ligand-induced inhibition at high concentration, which might yield bell-shaped synagics, is seen in many other fields including receptor studies (Trist & Leff 1985; Winding & Bindslev 1993; Bronnikov et al. 1999; Accomazzo et al. 2002; Hornigold et al. 2003; Schlee et al. 2006) and transport experiments with channels (Jow & Numann 1999; Murayama et al. 1999; Zwart & Vijverberg 2000; Hapfelmeier et al. 2003; Hong & Wang 2005), with pumps (Andersen et al. 2001; Bucher et al. 2005; Einholm et al. 2007), with co-transporters (Berthelot et al. 2005), with uniporters (Alpers 2005; Vieira et al. 2005), and in motor string formation (Hayashi et al. 2007).

DOI: 10.3402/bindslev.2008.5

3.1.2. A One-state Model to Analyze Ligand-dependent Auto-inhibition

Chapter 2 focused on simple inhibition by ligands different from the stimulatory agonist. In competitive type II and non-/un-competitive intervention, binding of an interventor ligand at a secondary site prevents either the binding of agonists at the primary site or the possible conformational change needed for activation of the receptive unit. This is the hetero-intervention model without co-lateral binding presented in sub-chapter 2.5. On the contrary, as described here, in auto-intervention just one ligand is present and this ligand can now bind at the same time to an orthosteric site as well as to a secondary binding site. That is, co-lateral binding is possible and efficacy and affinity interactions between sites may be invoked concomitantly with a single type of ligand (depicted in Section 2.6.3 and shown in Fig. 2.4-2). Again, I'll use the terms ligand, agonist, and substrate interchangeably.

3.1.3. Auto-inhibitory Concentration-binding and Dose-response Relationships

Three simple reaction schemes of auto-inhibition are shown in Fig. 3.1A, B, and C. The scheme in Fig. 3.1C is equal to the lower right quadrant of the four-pane one-state model (FP-OSM), shown as quadrant number 2 of Fig. 2.4. This scheme has simply three parameters due to microscopic reversibility (e.g., Colquhoun et al. 2004).

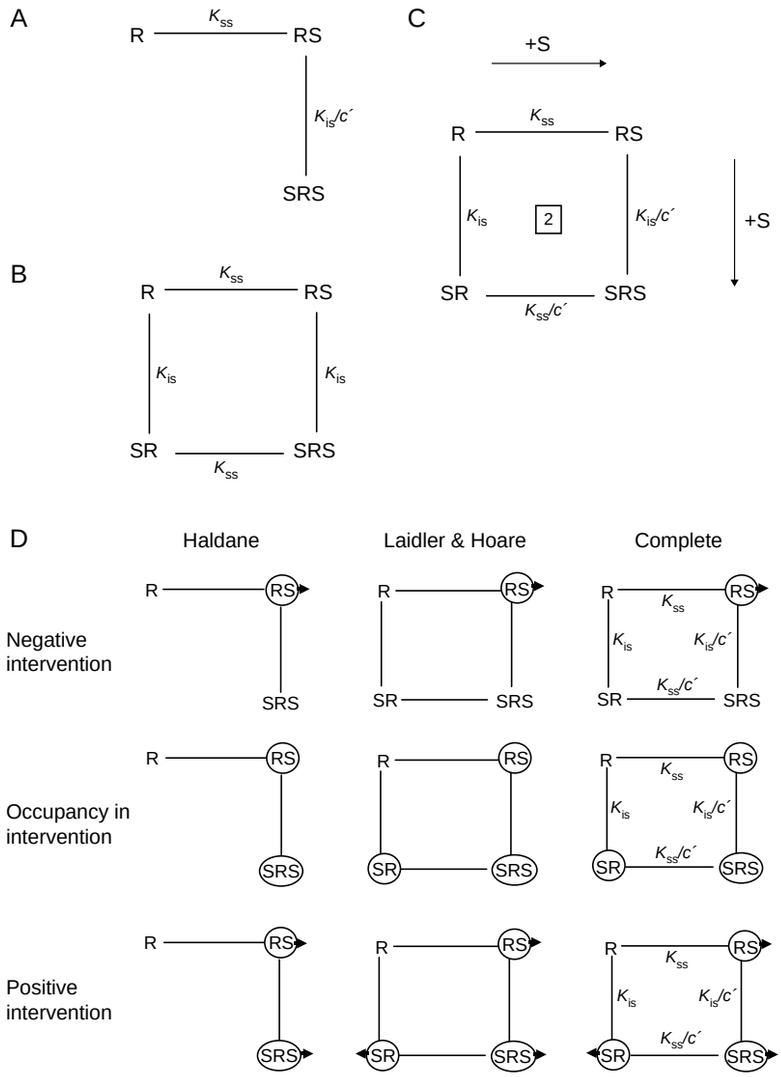

Figure 3.1. Forms of the auto-intervention one-state reaction scheme (AI-OSM). The models have two binding sites for the same ligand in a receptive unit R. (A) Haldane's model for substrate inhibition with the conformation SR missing (Haldane 1930). (B) Laidler-Hoare's model for substrate inhibition (Laidler & Hoare 1949). (C) The complete auto-intervention model. Panel D details the liganded species in negative and positive functional intervention and in intervention occupancy by circling the species. Function, activity, is indicated by arrowheads. Parameter c' is a co-lateral interaction coefficient in a single-ligand system. Parameter c' is ≥ 0 in the complete model.

The three reaction schemes in Fig. 3.1 have a receptive unit with a primary and a secondary binding site, where a ligand S can bind to both the primary site and to the secondary site simultaneously. As mentioned, this means that the binding of a ligand S is both co-lateral and mutually inclusive, as defined in sub-chapter 2.6. Binding of a ligand to the secondary site is assumed to prevent activation of the receptive unit, i.e., the receptor conformations SR and SRS are possible but not activatable (Fig. 3.1B + C). In such reaction schemes, only the RS conformation is ready to undergo the change to an active conformation, while SR and SRS are dead, functionally speaking. Such a behavior is designated 'auto-inhibition' or as 'negative co-operativity' by some, and in enzyme literature it is known as 'substrate-inhibition'.

In our present model of functional studies, since both conformations SR and SRS are non-active, the activity will always drop to zero at high enough agonist concentration, yielding a bell-shaped dose-response curve (Sections 3.2.2 and 3.2.3) (Haldane 1930; Laidler & Hoare 1949; Laidler 1956, 1958; Harper 1971).

3.1.4. Auto-intervention May Yield Bell-shaped Synagics and Changes in Apparent K_d

In auto-inhibition schemes as in Fig. 3.1, the agonist S behaves both as an agonist when binding to the primary site and as a negative interventor when it binds to the secondary binding site of a receptor and prevents function. Therefore, in functional studies, it turns out that the negative intervention always results in bell-shaped dose-responses, while in binding assays only the apparent dissociation constant differs from the real K_d. In models representing binding studies, the maximum occupancy is unaffected by auto-inhibition.

In receptor literature without a specific model, auto-inhibition is known as 'negative co-operativity', while in literature on carriers such as hemoglobin, 'positive co-operativity' is the characterizing term for augmented binding of O_2 at increasing O_2 concentration. Notice though, for carriers such as hemoglobin, as the concentration of the ligand increases, only the binding assay come into play where the result in comparison with simple **load** is an accelerated binding. Therefore, in the present context with one-state models, I suggest the term **auto-intervention**, which covers both changes in apparent K_d, shallow or accelerated binding in concentration-occupancy relations, and full-blown bell-shaped dose-effects of self-inhibition. Accordingly, throughout this text, where one-state models are assumed, I will use the term 'auto-intervention' and reserve similar terms as 'co-operative' or 'auto-modulation' for allosteric two-state models (ATSMs) (Chapters 7 and 15). Herewith, we can discriminate between one- and two-state models and indicate which type of model is employed in our analysis. Of note, terms such as 'auto-intervention', 'co-operativity', and 'auto-modulation' do not preclude positive effects. Thus, with a one-state model for O_2-binding to hemoglobin there is 'positive auto-intervention' revealed as steepened dose-response curves.

Usually the term 'negative co-operativity' does not cover for bell-shaped dose-responses, but rather for shallow synagics below the **load**-hyperbolic dose-response profile. Therefore, when analyzed by one-state models, a bell-shaped dose-response is also better designated with 'negative auto-intervention' or 'auto-inhibition'. Auto-intervention is either positive or negative.

The diagram in Fig. 3.1A is a scheme for 'auto-uncompetitive inhibition' and the diagram in Fig. 3.1B is a scheme for 'auto-non-competitive inhibition' (auto-ant-agonism). However, since both these reaction schemes are merely special cases of Fig. 3.1C, that is $c' \neq 1$ versus $c' = 1$, we can include Fig. 3.1A + B reaction schemes under the term 'auto-intervention'.

For auto-intervention as presented in Fig. 3.1, observe that the terms 'positive' and 'negative' are related directly to which conformations are active or non-active and not to parameter c', cf. for instance with top and bottom row in Fig. 3.1D.

3.1.5. Auto-intervention is Hetero-intervention-like

The reaction scheme of auto-intervention in Fig. 3.1C is also depicted in a quadrant of the FP-OSM reaction scheme shown earlier (Fig. 2.4-2). Furthermore, the system to be analyzed as shown in Fig. 3.1C, is a look-a-like of the hetero-intervention type reaction scheme shown in Fig. 2.4-1 and discussed in sub-chapter 2.5. Auto-intervention in one-state models is hetero-intervention-like because binding at the two sites are mutually inclusive and the co-lateral intervention constant c' is not necessarily equal to unity, which is also the case for the co-lateral intervention constant c of the hetero-interventory reaction scheme (cf Fig. 2.4-1). The novelty in the present auto-intervention one-state model, as mentioned above, is the possibility of the *same* ligand interacting with both a primary site and a secondary site, equal to co-lateral binding. Co-lateral binding was not possible in the one-state hetero-intervention reaction scheme (sub-chapter 2.5 and Fig. 2.4-1).

3.2. Formulation of Auto-intervention

3.2.1. Equations of Distribution for Simple Auto-intervention

For the formulation of a one-state reaction scheme with one-ligand and a two-site receptive unit with co-lateral binding as shown in Fig. 3.1C, I first list the possible receptor conformations and system constants:

R A receptive unit with two-binding-sites, an agonist S can bind both to a primary site (RS) as well as to a secondary site (SR).

As before, symbols for receptor species in reaction schemes may also stand for the concentration of receptors and receptor-complexes, thus, R is also [R].

$RS = R \cdot S/K_{ss}$ The agonist, S, is bound at a primary site in the receptive unit R. Tacitly, RS is also symbol for the active form R*S, which gives functional life to the receptor through a conformational isomerization. K_{ss} is the dissociation constant for S at the primary site.

$SR = R \cdot S/K_{is}$ SR is a complex of the receptive unit R with an agonist S bound at a secondary or intervention site. K_{is} is the dissociation constant for S at a secondary site. SR is assumed non-active.

$SRS = R \cdot (S/K_{ss}) \cdot (S \cdot c'/K_{is})$ SRS is the complex of a receptive unit with an agonist bound simultaneously to its primary and secondary sites. SRS is assumed non-active.

c' A co-lateral intervention constant for ligand binding at one site when the other site is already liganded with the same type of ligand. Compare parameters c and c' in Figs. 2.4-1 and 2.4-2.

As we shall soon experience, the assumption that both conformations SR and SRS are non-active is what leads to negative auto-intervention in the model.

To simplify matters, it is tacitly assumed that the reactive RS complex is in fast equilibrium with its activated state R*S, although this conformation of the receptive unit will not be included in our formulation. Since we operate with a one-state model for auto-intervention, explicit formulations of R* in general will not appear here; only later in TSMs (Chapters 5 and 7).

3.2.2. JBS's Formulation of Substrate Inhibition

Haldane[1] (1930, pp. 84–85) formulated the following equation in order to describe inhibition of enzymes at high substrate concentrations:

$$\frac{p}{e} = \frac{x}{K_1 + x + x^2/K_2}, \tag{3.1}$$

which may by transcribed to the terminology used in this book for the receptor reaction scheme as highlighted in Fig. 3.1A:

$$\frac{ar}{TR} = \frac{S/K_{ss}}{1 + S/K_{ss} + (S/K_{ss} \cdot S/K'_{is})} = \frac{S}{K_{ss} + S + S^2/K'_{is}}, \tag{3.2}$$

where p/e equals the fractional activity of actual response over total receptive units $= ar/TR$, $x = S =$ substrate or agonist concentration, $K_1 = K_{ss}$, and $K_2 = K'_{is}$. The parameter K'_{is} is the equilibrium dissociation constant for S at an intervention site when S is already bound to the orthosteric site. K'_{is} is also equal to $K_{is} \cdot 1/c'$ (cf Fig. 3.1A+C). The value of c' may thus be included in the new parameter K'_{is} (see Section 3.2.3).

The functional dose-response relation according to Eq. 3.2 is shown in Figs. 3.2A+B and 3.3A+B.

In his reaction scheme, Haldane disregarded a fourth conformation of the receptor, *viz.* SR, by only including the R, RS, and SRS forms of the enzyme, and therefore only included two equilibrium constants. Haldane's model resembles un-competitive ant-agonism, where binding to the secondary site is only possible when the primary site is liganded (Section 2.5.4) (Segel 1975, 1993, pp. 136–143).

Haldane's scheme is an ordered reaction scheme with a single type of ligand (see Chapter 6).

Lineweaver and Burk expanded the Haldane scheme slightly by allowing an exponentiation to a higher order than 2 (Lineweaver & Burk 1934; Nayyar & Glick 1956).

3.2.3. A More Complete Model for Auto-intervention in Functional Assays

Although assuming that $c' = 1$, a more complete distribution equation in **functional** assays of auto-intervention than that of Haldane can be formulated by including the SR conformation of the reaction scheme as shown in Fig. 3.1B. Its dose-response equation reads:

$$\frac{ar}{TR} = \frac{S/K_{ss}}{1 + S/K_{ss} + S/K_{is} + (S/K_{ss} \cdot S/K_{is})} = \frac{S}{K_{ss} + S + S \cdot K_{ss}/K_{is} + S^2/K_{is}}, \tag{3.3}$$

with a denominator representing all four receptor conformations. In 1949 (Laidler & Hoare), a similar equation had already been derived tacitly assuming parameter c' to be 1.

[1] JBS Haldane held a professorship in physiology and was a reader in biochemistry when his book 'Enzymes' was published. He is one of my favorite milestone-idols in natural sciences, including population genetics. Among many other qualities, he was physically strong, smart, stubborn, sturdy, Stalinist, super-kind humanist, and bloody-minded. Quite an impossible man with a ferocious memory and intellect. JBS is decently depicted in a biography by Roland W. Clark (1968).

Plots of Laidler and Hoare's dose-response curves for function are shown in Figs. 3.2C+D and 3.3C+D. The Haldane and Laidler-Hoare dose-response curves in functional studies are always bell-shaped. In both schemes when $K_{is}/K_{ss} > 1000$, the maximal response approaches 100% and there is a broadening of the maximum plateau as the ratio increases (Fig. 3.3 panels A+B and C+D). When the ratio K_{is}/K_{ss} falls below 1000, the two legs of the bell merge and the maximum response falls towards zero (Fig. 3.2 panels A+B and C+D). Furthermore, as K_{ss} increases separately, the left leg of the bell is right-shifted (Figs. 3.2C and 3.3C), whereas when K_{is} increases separately, the right leg of the bell moves to the right (Figs. 3.2D and 3.3D). When both K_{ss} and K_{is} increase (move to the right) in a fixed ratio, the bell moves unchanged to the right as well (not shown).

Compared with the Laidler-Hoare scheme, Haldane's omission of SR does not dramatically alter the shape of the negative auto-intervention curve as long as $K_{is}/K_{ss} > 100$ (Figs. 3.2A+B versus C+D and 3.3A+B versus C+D).

Notice, conformations involving the term S/K_{is} do not appear in the nominator of functional expressions (Eqs. 3.2 and 3.3), as they are considered non-functional conformations, while in binding studies, these terms must appear in the nominator! Therefore, the above equations are valid for functional studies, but not for binding studies.

So far, we have assumed that c' is equal to 1, meaning that $K'_{is} = K_{is}$ or $K^{ss}_{is} = K_{is}$. See Box 2.1 on parameter sub- and superscripts.

3.3. Completion of the Simple Auto-intervention Model

3.3.1. Auto-intervention for Function with Intervention Constant $c' \neq 1$

It is time to derive a formulation of the complete distribution function for the auto-inhibition one-state reaction scheme by including a co-lateral intervention parameter that deviates from unity, $c' \neq 1$, as presented for functional studies in Fig. 3.1C. I re-emphasize that the co-lateral intervention constant c in the hetero-intervention reaction schemes is now replaced with c apostrophe (c'), just to indicate that they are two different parameters in two different reaction schemes. The apostrophed intervention constant c' is for two

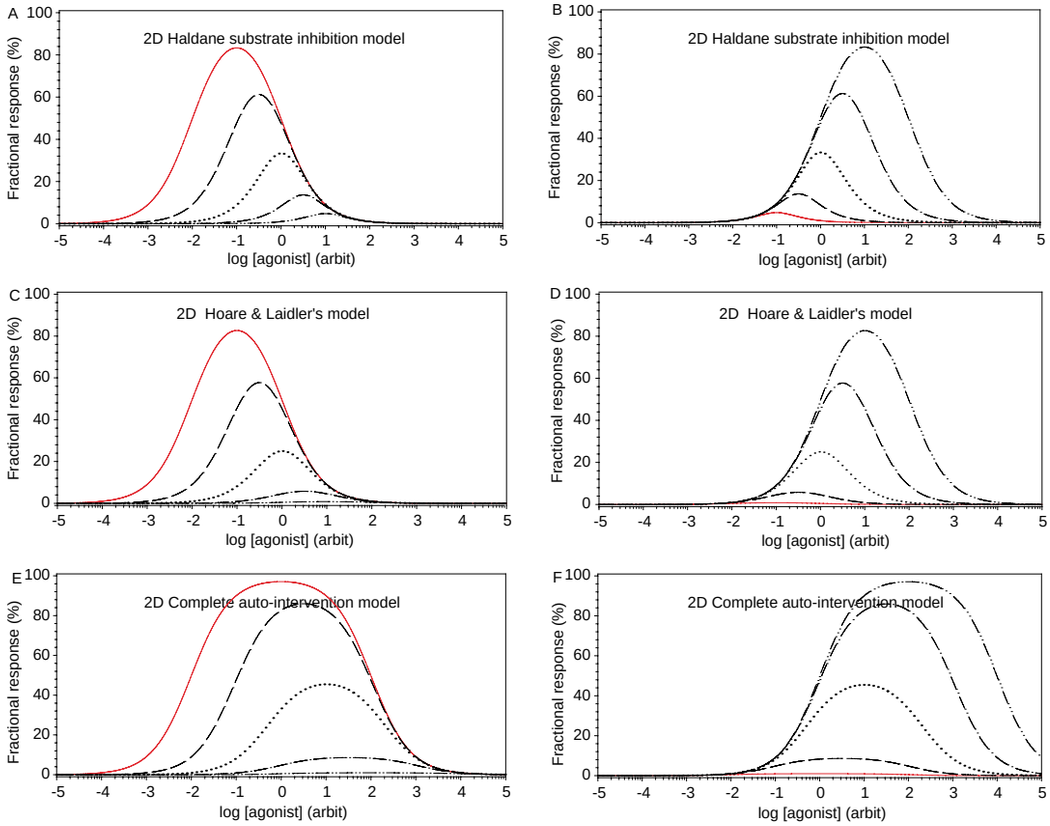

Figure 3.2. Functional dose-response curves of the three reaction schemes in Fig. 3.1. In A, C, and E, K_{ss} vary between 10^{-2} (—) and 10^{2} (– ·· –) in five steps by a factor 10, while $K_{is} = 1$. In B, D and F, K_{is} vary between 10^{2} (—) and 10^{-2} (– ·· –) in five steps by a factor 10, while $K_{ss} = 1$. Co-lateral coefficient c' is 1 in A, B, C, and D, and c' is 0.01 in E and F.

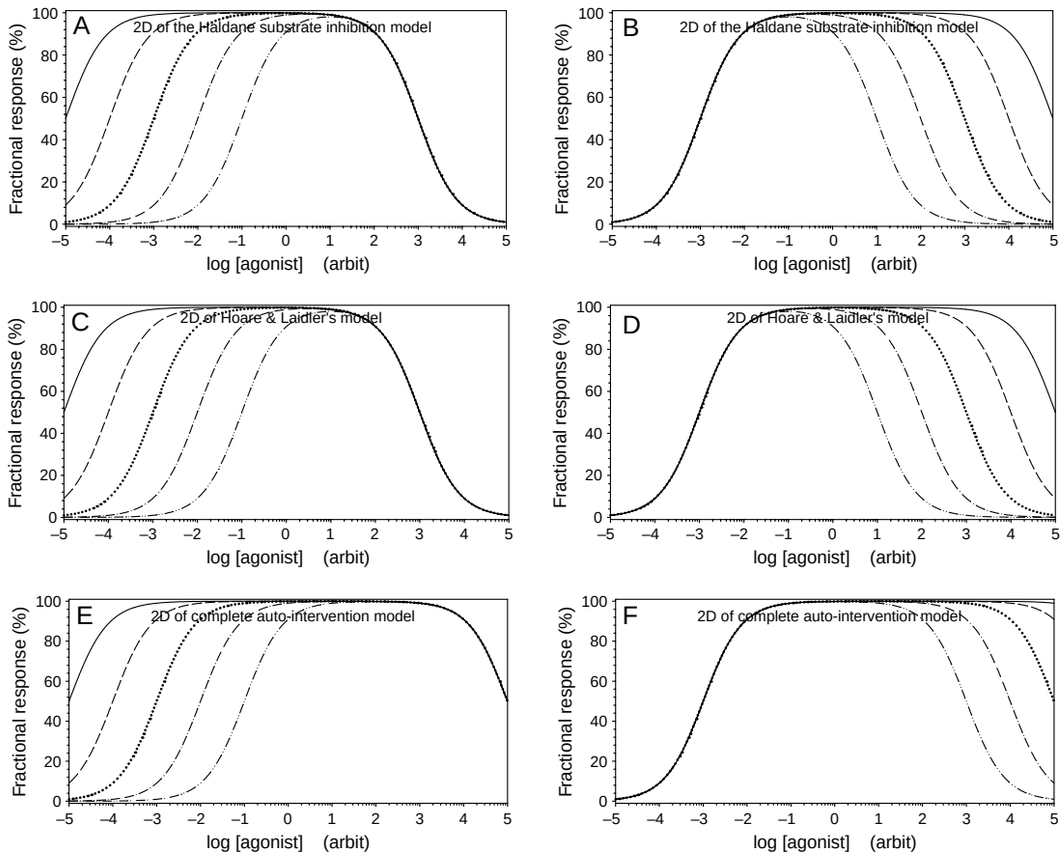

Figure 3.3. Functional dose-response curves of the three negative intervention schemes in Fig. 3.1D. In A, C, and E, K_{ss} vary between 10^{-5} (—) and 10^{-1} (– ·· –) in five steps by a factor 10, while $K_{is} = 1000$. In B, D, and F, K_{is} vary between 10^{5} (—) and 10^{1} (– ·· –) in five steps by a factor 10, while $K_{ss} = 0.001$. Co-lateral coefficient c' is 1 in A, B, C, and D, and c' is 0.01 in E and F.

identical ligands (Figs. 2.4-2 and 3.1C), whereas the intervention constant c, without an apostrophe, is for two different ligands (Fig 2.4-1).

Furthermore, I continue formulations by still employing dissociation constants instead of association constants in order to compare with formulations by Haldane and Laidler-Hoare in Sections 3.2.2 and 3.2.3.

For an equation of dose-response for the complete **functional** auto-intervention scheme (Fig. 3.1C), with the terminology given in Section 3.2.1, you should get:

$$\frac{ar}{TR} = \frac{S/K_{ss}}{1 + S/K_{ss} + S/K_{is} + (S/K_{ss}) \cdot (S \cdot c'/K_{is})}, \quad (3.4)$$

which may be rewritten to:

$$= \frac{S}{S + S \cdot K_{ss}/K_{is} + S^2 \cdot c'/K_{is} + K_{ss}}. \quad (3.5)$$

The dose-response curves of this equation for the complete reaction scheme of negative auto-intervention is depicted in Figs. 3.2E + F and 3.3E + F. When an agonist is also a negative interventor in its own transduction pathway, it can be both a stimulator at low concentrations and an auto-inhibitor at higher concentrations. Again, the negative intervention is due to non-active conformations with S bound at the i-site.

The manner in which the three parameters K_{ss}, K_{is}, and c' affect the bell-shaped dose-responses is written up in Table 3.1A.

The distribution function in Eq. 3.5 of a negative complete auto-intervention model for activity was derived in the 1950s (Segal et al. 1952; Botts & Morales 1953; Laidler 1956, 1958, pp. 77–79), and later even more elaborately analyzed by Harper (1971). Modern versions may be found in Shou (2005).

3.3.2. Other Model Approaches to Experimentation Yielding Bell-shaped Synagics

Mathematical modeling and parameter determination for bell-shaped synagics is possible with either a double-**load** or a double-Hill formulation (see, e.g., Szabadi 1974; Jarv et al. 1993; Rovarti & Nicosia 1994; Tucek et al. 2002; Griffen et al. 2003; Hornigold et al. 2003). However, a mechanistic interpretation of obtained parameter values is meaningless with these approaches. Therefore, let us return to aspects of the auto-intervention model.

Table 3.1A. Function in three **negative** intervention models. The related reaction schemes are shown in the upper row of Fig. 3.1D. All dose-responses of the negative intervention models are **bell-shaped** (see Fig. 3.3A–C). As listed in the table, the bell height and the broadness of the bell-plateau are altered by varying one of three parameters, K_{ss}, K_{is}, and c' indicated in parentheses, while keeping the others at unity. Haldane's model is described in Eq. 3.2, Laidler–Hoare's model (L&H) is described in Eq. 3.3, and the complete intervention model is described in Eqs. 3.4 and 3.5.

Model	Parameter value	R_{max} (K_{ss}) (%)	Bell move	R_{max} (K_{is}) (%)	Bell move	R_{max} (c') (%)	Bell move
Haldane	$<<1$	100	Down to the Right*	0	Up to the Right*	35	No
	$=1$	35		35			
	$>>1$	0		100			
L&H	$<<1$	100	Down to the Right*	0	Up to the Right*	25	No
	$=1$	25		25			
	$>>1$	0		100			
Complete	$<<1$	100	Down to the Right*	0	Up to the Right*	50	Down Left*
	$=1$	25		25		25	
	$>>1$	0		100		0	

*Lower values of K_{ss} and c' and increasing values of K_{is} result in a broadening of the bell-plateau (see also Fig. 3.3).

3.3.3. Auto-intervention for Binding with Intervention Constant c′ ≠ 1

Next, let us look at the reaction scheme for auto-intervention in a concentration-binding regime, where receptive units with two bound ligands count twice (Fig. 3.1C). The fractional binding in this reaction scheme has the following equation:

$$\frac{\text{occupancy}}{\text{total}} = \frac{S/K_{ss} + S/K_{is} + 2\cdot(S/K_{ss})\cdot(S\cdot c'/K_{is})}{1 + S/K_{ss} + S/K_{is} + 2\cdot(S/K_{ss})\cdot(S\cdot c'/K_{is})}, \tag{3.6}$$

which also reads:

$$\frac{\text{occupancy}}{\text{total}} = \frac{S}{S + \dfrac{K_{ss}}{1 + K_{ss}/K_{is} + 2\cdot S\cdot c'/K_{is}}}. \tag{3.7a}$$

The terms multiplied by a factor 2 take care of the double-liganded receptive units.

Similar equations for binding in the Laidler–Hoare and Haldane's reaction schemes are as follows:

$$\frac{\text{occupancy}}{\text{total}} = \frac{S}{S + \dfrac{K_{ss}}{1 + K_{ss}/K_{is} + 2\cdot S/K_{is}}}. \tag{3.7b}$$

for the Laidler–Hoare scheme shown in Fig. 3.1B, and:

$$\frac{\text{occupancy}}{\text{total}} = \frac{S}{S + \dfrac{K_{ss}}{1 + 2\cdot S/K'_{is}}}. \tag{3.7c}$$

for the Haldane scheme shown in Fig. 3.1A.

Examples of plots for these concentration-binding relationships are shown in Figs. 3.4A + B and 3.5A + B for Haldane, Figs. 3.4C + D and 3.5C + D for Laidler-Hoare, and Figs. 3.4E + F and 3.5E + F for the complete auto-intervention scheme. Table 3.1B gives a summary of the effects on binding steepness by varying one of the three parameters K_{ss}, K_{is}, and c'.

When occupancy is by a radioactive isotope and displacement is by an identical cold isotope, Eq. 3.7*a* is expanded and can demonstrate the so-called 'low-dose hook-effect' (see sub-chapter 3.4).

3.3.4. Positive Auto-intervention in Functional Studies

Positive auto-intervention of function is described by a set of equations similar to Eqs. 3.7*a–c* for binding with the sole modification that the factor '2' is omitted. Therefore, plots of positive functional auto-intervention are almost identical to plots of the concentration-binding relations shown in Figs. 3.4 and Fig. 3.5. The steepness of the dose-response relations are determined by the value of parameters K_{ss}, K_{is}, and c'. The effects of varying one of the three parameters on this dose-response steepness are quantified by the Hill coefficient n_H in Table 3.1C.

3.3.5. Conversion of Hetero-intervention into a One-state Substrate Inhibition Model

You should realize that in an auto-intervention model for substrate inhibition, the dose-response formula for a ligand S that is both an agonist at an s-site and a negative interventor at an i-site, is in principle similar to dose-response equations for hetero-intervention in a mutually exclusive one-state model (ME-OSM). Here an agonist S can only bind to an s-site and a different ligand, I, can only bind to an i-site on the receptive unit (see sub-chapter 2.6.3 and Section 3.1.5). Thus, the formula for negative functional hetero-intervention (Eq. 2.17 in sub-chapter 2.5), may easily be re-formulated to functional auto-intervention by simply substituting 'I' with 'S', keeping 'i' in the subscripts first position, and in the second subscript position replacing 'i' with 's' at relevant positions in the pertinent equations. This, for instance, results in K_{ii} transformed to K_{is}. Further, c is now c'. With these changes, Eq. 2.17 is equal to Eq. 3.4.

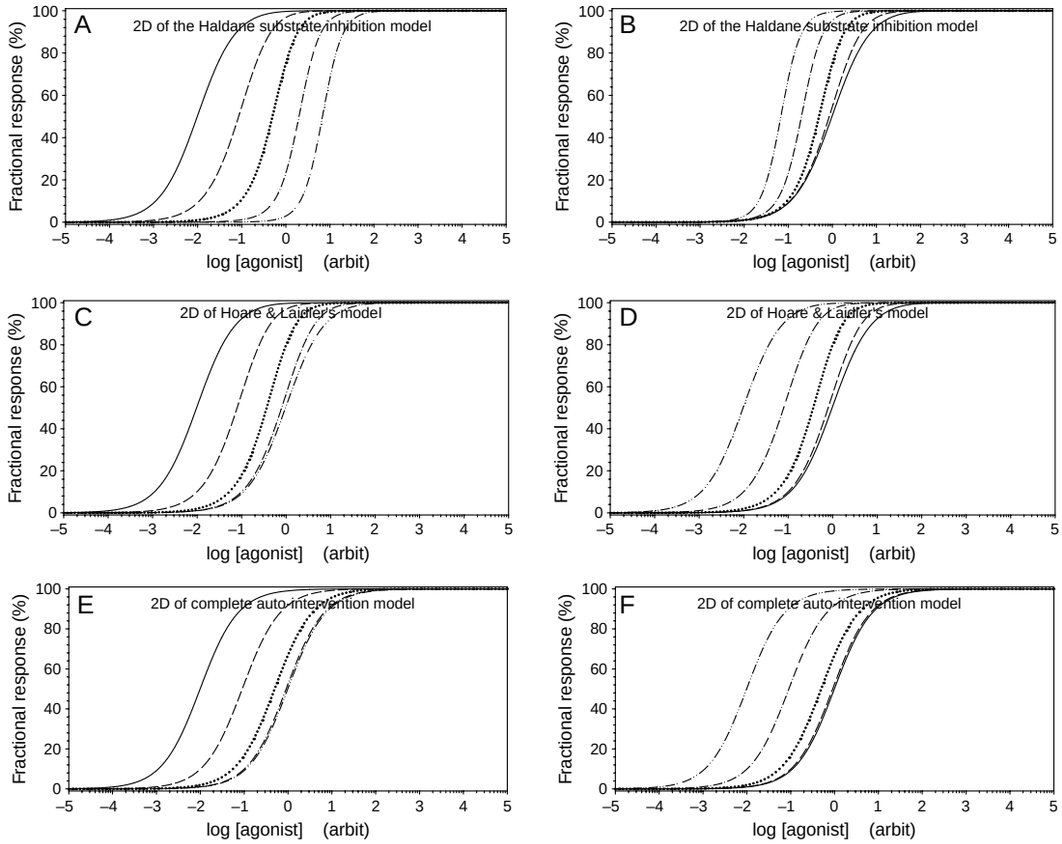

Figure 3.4. Binding concentration-occupancy curves of the three intervention schemes in Fig. 3.1D. In A, C, and E, K_{ss} vary between 10^{-2} (—) and 10^{2} (– ·· –) in five steps by a factor 10, while $K_{is} = 1$. In B, D, and F, K_{is} vary between 10^{2} (—) and 10^{-2} (– ·· –) in five steps by a factor 10, while $K_{ss} = 1$. Co-lateral coefficient c' is 1 in A, B, C, and D, and c' is 0.01 in E and F.

3.3.6. Switch of Hetero-intervention in 3-D to Auto-intervention in 2-D

Three-dimensional surface-plots for the functional version of the hetero-intervention model are shown in Fig. 2.11. In experiments where a mixture of substrate and interventor in a fixed ratio of concentrations is used to change ligand concentration, the surface-plots change into 2-D plots, as shown by the arrows in Fig. 2.11. Hence, hetero-intervention in 3-D in Fig. 2.11 is converted to auto-intervention in 2-D as in Figs. 3.2 and 3.3. The conclusion from Figs. 2.11 and 3.2-3.3 is that auto-intervention is a special case of the more general hetero-intervention scheme.

3.3.7. Conclusions on the Auto-intervention Behavior

The behavior of the auto-intervention reaction scheme for concentration-binding and of the auto-intervention reaction scheme for the dose-response relation is summarized in Table 3.1A, B, and C while examples of the impact of varying single parameter values of K_{ss}, K_{is}, or c' in the functional scheme are shown in Figs. 3.2 and 3.3 and for the binding scheme in Figs. 3.4 and 3.5.

For functional dose-response curves, all the fractional response curves display bell-shaped behavior. The drop in activity at high ligand concentrations for the dose-response curves is simply due to the fact that neither the SR nor the SRS conformations of the receptive units contribute to the activity (Figs. 3.2 and 3.3).

As the value of c' decreases below unity, the co-lateral intervention parameter c' has a broadening effect on the bell-shaped dose-responses (compare panel E with panels A and C and panel F with panels B and D in Figs. 3.2 and 3.3). Parameter c' also determines the steepness of concentration-occupancy and positive auto-intervention dose-responses in functional relations. Compare these effects of c' with the effects of the same parameter in the functional homotropic two-state model (HOTSM) (Chapter 7). The effects of constant c' may also be compared with the effects of the similar parameter c in the functional hetero-intervention model (sub-chapter 2.5), and in dose-responses of the ATSM described in Chapter 7.

All the fractional concentration-binding curves increase continuously towards unity as the ligand concentration increases and the apparent dissociation constant is dependent on the relation between K_{ss}, K_{is}, and c', as

Table 3.1B. Occupancy in three intervention models. The related reaction schemes are shown in the middle row of Fig. 3.1D. All dose-binding curves of the occupancy intervention models reach maximal binding with increasing ligand concentration (see Figs. 3.4A–C). As listed in the table, the steepness of curves and the position on the concentration axis are altered by varying one of three parameters, K_{ss}, K_{is}, and c' indicated in parentheses, while keeping the others at unity. Haldane's model is described in Eq. 3.7*c*, Laidler–Hoare's model (L&H) is described in Eq. 3.7*b*, and the complete intervention model is described in Eq 3.7*a*.

Model	Parameter	n_H (K_{ss})	Curve move	n_H (K_{is})	Curve move	n_H (c')	Curve move
Haldane	$<<1$	1.0	Right	2.0	Right	1.468 ($c'=0$)	No
	$=1$	1.468		1.468			
	$>>1$	2.0		1.0			
L&H	$<<1$	1.0	Right	1.0	Right	1.267 ($c'=1$)	No
	$=1$	1.267		1.267			
	$>>1$	1.0		1.0			
Complete	$<<1$	1.0	Right	1.0	Right	1.0	Left
	$=1$	1.267		1.267		1.267	
	$>>1$	1.0		1.0		2.0	

indicated in Table 3.1 and shown by examples in Figs. 3.4 and 3.5.

When the hetero-intervention reaction scheme is conducted with a mixture of agonist and interventor in a fixed ratio (Fig. 2.11), the result is equal to the auto-intervention dose-response relationship as shown in Figs. 3.2 and 3.3 (see Sections 3.3.4 and 3.3.5).

3.4. The 'Low-dose Hook Effect'

In concentration-occupancy studies, there are two hook effects–the 'high' and the 'low' hook effect.

In binding studies, observed convex bell-shaped relations are described in the literature as a 'high-dose hook effect' when using high doses of antigen in so-called 2-site

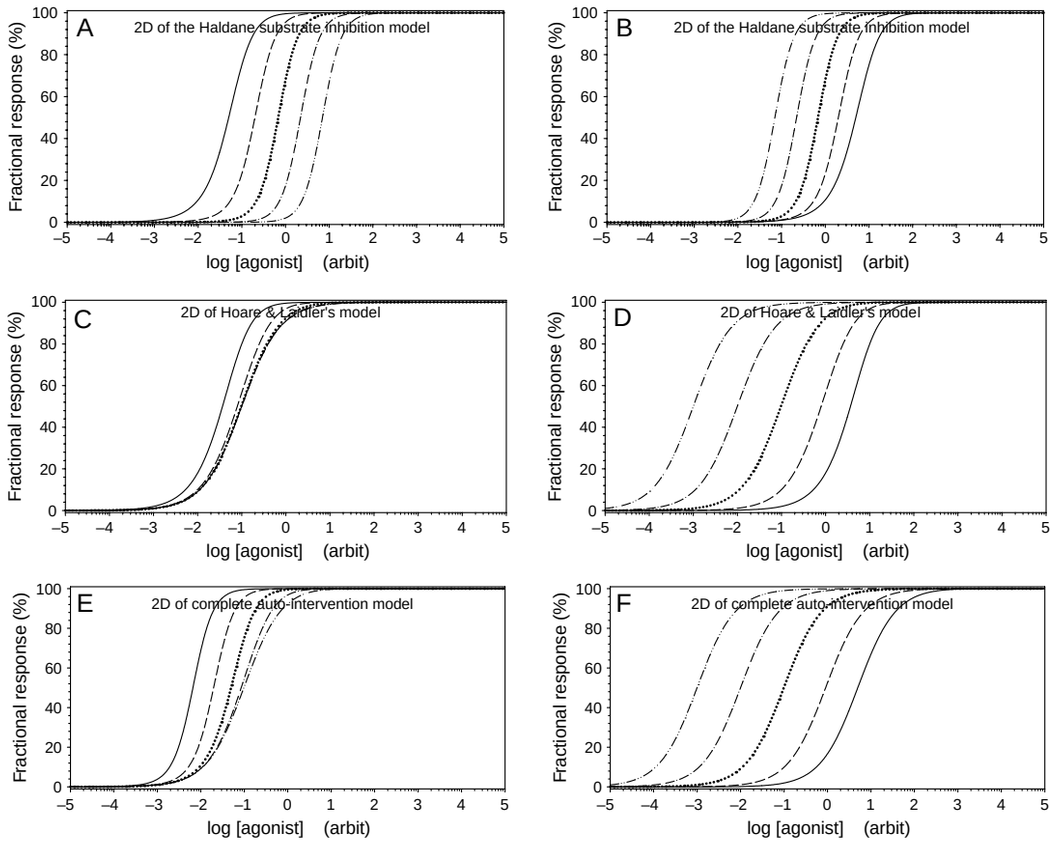

Figure 3.5. Functional dose-response curves of the three positive intervention schemes in Fig. 3.1D. In A, C, and E, K_{ss} vary between 10^{-1} (—) and 10^{3} (– ·· –) in five steps by a factor 10, while $K_{is}=0.1$. In B, D, and F, K_{is} vary between 10^{1} (—) and 10^{-3} (– ·· –) in five steps by a factor 10, while $K_{ss}=10$. Co-lateral coefficient c' is 1 in A, B, C, and D, and c' is 0.01 in E and F.

Table 3.1C. Function in three **positive** intervention models. The related reaction schemes are shown in the lower row of Fig. 3.1D. All dose-responses of the functional form of positive intervention models reach maximal activation with increasing ligand concentration (see Fig. 3.5A-C). As listed in the table, the steepness of curves and the position on the concentration axis are altered by varying one of three parameters, K_{ss}, K_{is}, and c' indicated in parentheses, while keeping the others at unity. By removing a factor 2 from the following three equations: Haldane's model is described in Eq. 3.7*c*, Laidler-Hoare's model (L&H) is described in Eq. 3.7*b*, and the complete intervention model is described in Eq. 3.7*a*.

Model	Parameter	n_H (K_{ss})	Curve move	n_H (K_{is})	Curve move	n_H (c')	Curve move
Haldane	$<<1$	1.0	Right	2.0	Right	1.364 ($c'=0$)	No
	$=1$	1.364		1.364			
	$>>1$	2.0		1.0			
L&H	$<<1$	1.0	Right	1.0	Right	1.184 ($c'=1$)	No
	$=1$	1.184		1.184			
	$>>1$	1.0		1.0			
Complete	$<<1$	1.0	Right	1.0	Right	1.0	Left
	$=1$	1.184		1.184		1.184	
	$>>1$	1.0		1.0		2.0	

immuno-radio-metric assays (2-site IRMA) curves (Fig. 3.6) (Miles et al. 1974; Rodbard 1988; Leboeuf et al. 2006, and references therein). Miles and coworkers first suggested an explanation for the 'high-dose hook effect' seen in 2-site IRMAs. At high antigen concentration, a non-specific low-affinity binding of the antigen to the solid-phase antibody in a first reaction may interfere with available labeled antibody in a second step, thus reducing the number of labeled antibodies present for binding to insolubilized antigen (Miles et al. 1974; Miles 1975).

Another 'hook' relation is seen in homologous displacement studies in radio-immuno assays (RIAs). This other type of bell-shaped displacement curve is sometimes observed at low concentrations of cold ligand used to displace a homologous radio-ligand (Fig. 3.7) (Matsukura et al. 1971). I call this response the 'low-dose hook effect'.

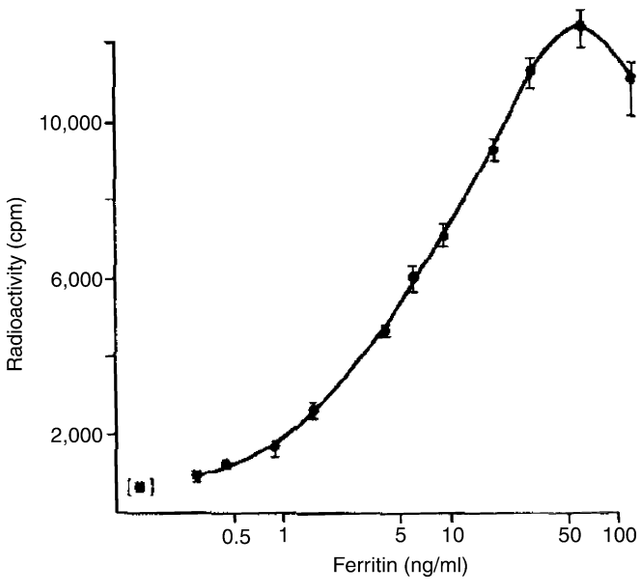

Figure 3.6. High-dose hook effect. This dose-response relation is the first described example of a 'high-dose hook effect' in a 2-site immuno-radiometric assay (2-site IRMA; Miles et al. 1974, Fig. 6A). See text for an explanation. Reproduced with permission.

An explanation for the 'low-dose hook effect' was given by Swillens et al. (1995) as due to positive interaction between two binding sites resulting in bell-shaped displacement curves (Fig. 3.8). The Swillens scheme is developed further in Sections 3.4.2–3.4.4.

Non-equilibrium condition is another explanation for low-dose hook effects, as formulated by Lazareno and coworkers (Lazareno & Birdsall 1995; Lazareno et al. 2000) and may be an explanation for the observed hooks in Fig. 3.7. Non-equilibrium conditions were likewise suggested as an explanation for an observed low-dose hook effect in a heterologous setup with KT5720 as interventor in the binding of muscarinic toxin MT-7 (Onali et al. 2005) to the M1 muscarinic subtype receptor (Fig. 3.9) (Fruchart-Gaillard et al. 2006, Fig. 8A). Meanwhile, a two-site hypothesis for the 'low-dose hook effect', to be discussed and analyzed in more details in the following sections, was not tested by these authors.

Note, the heterotropic association-dissociation bell-shaped relations, described by Monod and coworkers (Monod et al. 1963; Fig. 3), are a different story.

3.4.1. Low-dose Hook Effects

In RIA-displacement studies, an increase instead of a decrease in radio-ligand binding is sometimes observed at the start of increasing concentrations of cold isotope displacer. Thus, at concentrations in proximity to the common dissociation constant for a homologous and non-radioactive ligand used as a displacer, an increase is sometimes observed in bound radio-activity before a drop in bound radio-activity as concentrations of the cold isotope are increased. Swillens and co-workers have presented a simple reaction scheme involving two

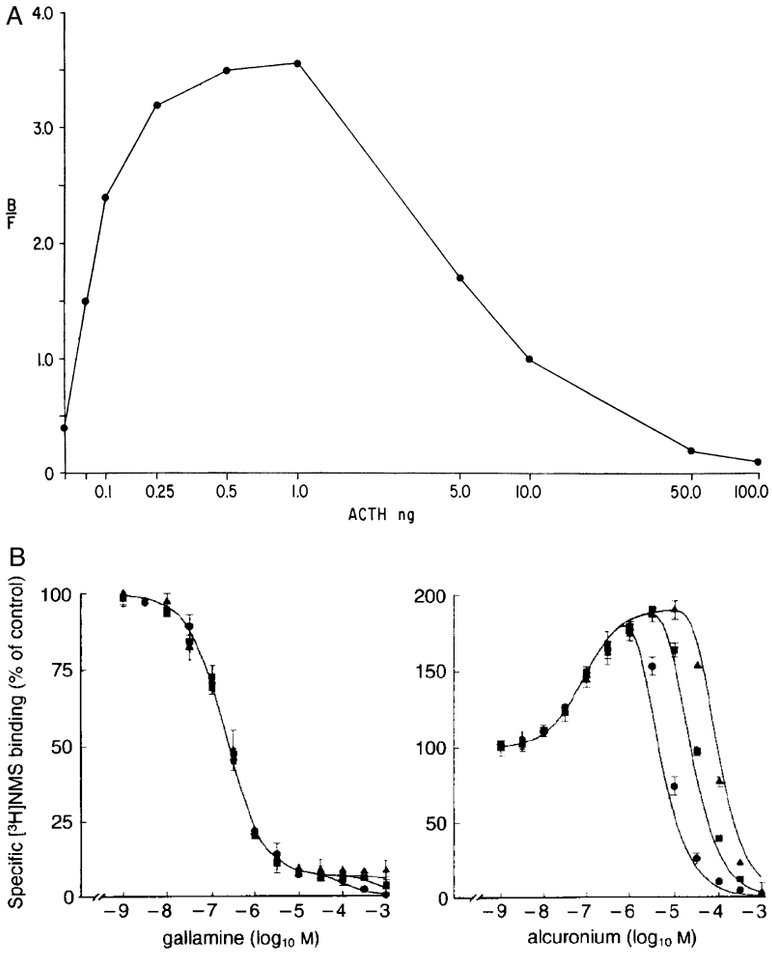

Figure 3.7. Low-dose hook effects. (A) Matsukura et al. (1971, Fig 2) as some of the first observed what looks like a low-dose hook effect in radioactive displacement studies. (B) Bell-shaped displacement of tracer NMS by cold gallamine or alcuronium. Tucek and Proska (1995, Fig. 2) with permission.

interacting binding sites, which for certain parameter values behave as described above (Swillens et al. 1995).

3.4.2. Swillens' Scheme

According to Swillens et al. (1995), the reaction scheme for a radio-active ligand symbolized as S^* and binding to a two-sited receptive unit R where the sites interact has the following formulation when transcribed to our terminology:

$$R + 2S^* \overset{A_s}{\rightleftharpoons} RS^* + S^* \text{ (or } S^*R + S^*) \overset{A_s \cdot c'}{\rightleftharpoons} S^*RS^*$$

where A_s is the association constant for binding either the cold isotope S or the tracer S^* to the receptive unit R, and $A_s \cdot c'$ is a combined association constant and an auto-intervention constant. Constant c' is an interaction coefficient for enhancement or attenuation in binding affinity for a second ligand following binding of a first ligand. The constant $A_s \cdot c'$ is again the same for both tracer and cold displacer molecule. For training purposes, I have replaced dissociation constants and switched to association constants. The above reaction scheme is the same as a compact version of the auto-intervention schemes presented in sub-chapter 3.3 (Fig. 3.1), but now with association constants. In the above version of the auto-intervention scheme, it is undecided whether binding is ordered or random. If binding at a primary site takes place before binding at the secondary site, it is an ordered reaction (Fig. 3.1A). See Chapter 6 for more on ordered and random reaction schemes.

Naturally, there are other examples of models with 'hook-effects' for a single ligand. One example with hook effects for a single ligand is Kühl's minimal recovery model (sub-chapter 3.7), where rate constants are invoked instead of, as here, Swillens et al.'s multi-sited interaction.

3.4.3. Formulation of Swillens' Scheme for Low-dose Hook Effects

The complete reaction scheme for the displacement of radio-active ligands with cold isotope at a two-sited

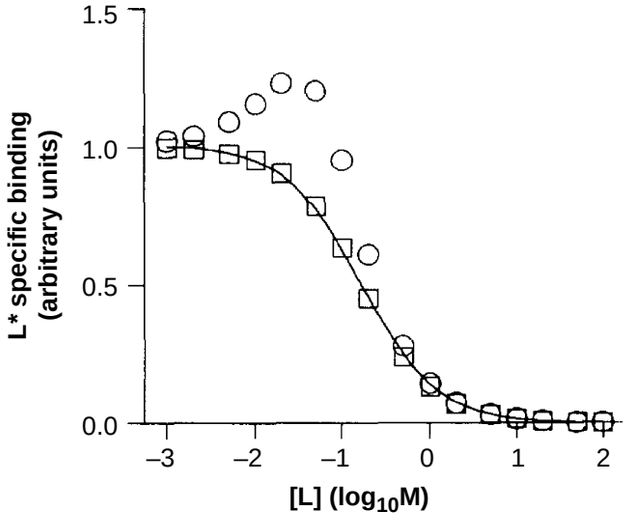

Figure 3.8. Theoretical low-dose hook effect. Assuming a two-sited receptive unit with 'positive co-operativity' between sites, radioactive binding displacement experiment may display a 'low-dose hook effect' at low to moderate concentrations of the radioactive ligand as demonstrated by Swillens et al. (1995; Fig. 3b). See subchapter 3.4 for further details. Reproduced with permission.

receptor system is shown in Fig. 3.10, and includes the possibility of site interaction, $c' \neq 1$. Compare Fig. 3.10 with a similar heterologous four-pane one-state reaction scheme in Fig. 2.4.

As mentioned above, we assume that the association constants for both tracer and cold isotope are the same on either site, i.e., $A_{ss*} = A_{ss}$ and $A_{is*} = A_{is}$, and binding is random. In case the binding is ordered, conformations SR and S*R will disappear from the scheme in Fig. 3.10, and the reaction will resemble an un-competitive reaction, but in principle with two identical ligands, tracer and cold isotope.

Now we will further assume that A_{ss} is also equal to A_{is} and derive the related equation.

The equation for displacement of a radioactive isotope, S^*, by cold isotope, S, in a random four-pane one-state scheme (Fig. 3.10), only contains the liganded conformations with cold isotope in its denominator. Thus, for $A_{ss} = A_{is}$, the sum:

$$\begin{aligned}\text{of unlabeled species} &= \mathrm{UL}_{s=i} = 1 + 2\cdot S\cdot A_{ss} + (S\cdot A_{ss})^2\cdot c',\\ \text{in the nominator} &= \mathrm{N}_{s=i}, \;= 2\cdot S^*\cdot A_{ss}\cdot(1 + S^*\cdot A_{ss}\cdot c'\\ &\quad + S\cdot A_{ss}\cdot c'), \text{ and}\\ \text{in the denominator} &= \mathrm{D}_{s=i} \;= \mathrm{UL}_{s=i} + \mathrm{N}_{s=i},\end{aligned}$$

and the fractional bound tracer is:

$$\frac{\text{bound tracer}}{\text{total ligand}} = \frac{\mathrm{N}_{s=i}}{\mathrm{UL}_{s=i} + \mathrm{N}_{s=i}}. \tag{3.8}$$

S^* will be fixed for the single experiment, while S varies. The displacement of tracer for $A_{ss} = A_{is}$, is shown in Fig. 3.11. As shown in panel 3.11A, for certain values of association constant A_{ss} and of coupling coefficient c' and the level of initial tracer occupancy, there is a 'hook'

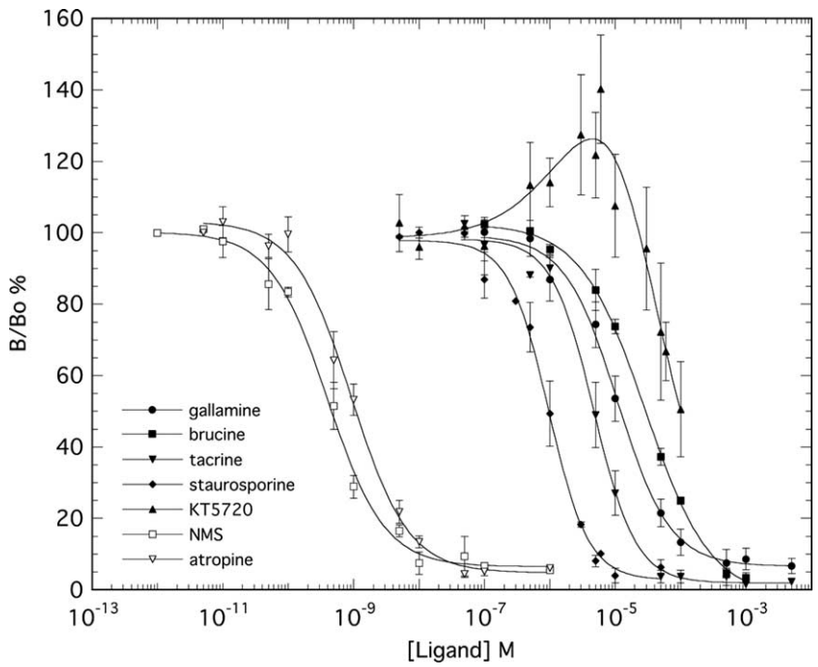

Figure 3.9. Non-equilibrium may explain 'low-dose hook effects'? The observed low-dose bell-shaped relation could possibly be explained by a heterologous displacement in a one-state intervention model (see text). However, the authors interpreted the observed hook effect as a non-equilibrium phenomenon. From Fruchart-Gaillard et al. (2006, Fig. 8A) with permission.

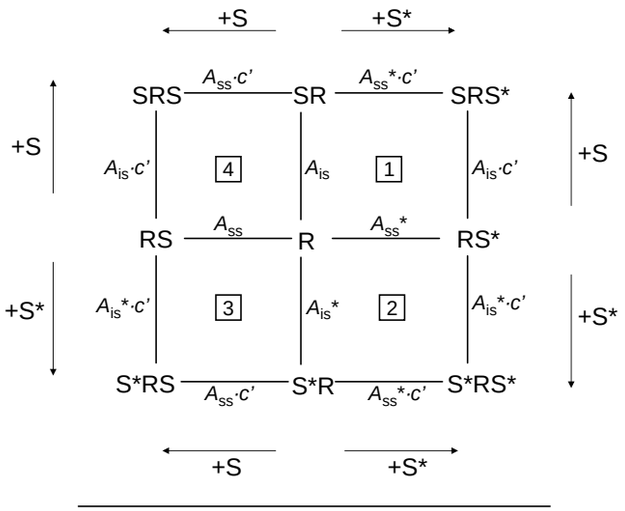

Figure 3.10. Reaction scheme for ligand displacement of tracer by cold isotope. The reaction scheme is a two-sited one-state model in an isotopic four-pane model (I-FP-OSM). The scheme may explain 'low-dose hook effects' seen in RIA assays.

on the binding displacement-curve as the concentration of cold isotope is raised.

The 3-D surface plot in Fig. 3.11B is only realistic in theory, where the concentration of cold isotope may be assumed to change separately either at the primary site, s-site, following the *x*-axis or at the intervention site, i-site, following the *y*-axis. In real life, the relationship will follow a cut through the surface topology along the indicated arrow in the x–y plane, yielding curves as shown in the 2-D graph in Fig. 3.11A.

Next, in the isotopic FP-OSM (I-FP-OSM; Fig. 3.10), we assume that $A_{ss} \neq A_{is}$, therefore its fractional occupancy equation will be slightly different from Eq. 3.8. The complete I-FP-OSM for binding in Fig. 3.10 now has the following sum:

$$\begin{aligned}
\text{of unlabeled species} &= \mathrm{UL}_{s\neq I} \\
&= 1 + \mathrm{S}\cdot A_{ss}\cdot(1 + \mathrm{S}\cdot A_{is}\cdot c') + \mathrm{S}\cdot A_{is}, \\
\text{in the nominator} &= \mathrm{N}_{s\neq I} \\
&= \mathrm{S}^*\cdot A_{ss}\cdot(1 + 2\cdot\mathrm{S}^*\cdot A_{is}\cdot c' \\
&\quad + 2\cdot\mathrm{S}\cdot A_{is}\cdot c') + \mathrm{S}^*\cdot A_{is}, \\
\text{in the denominator} &= \mathrm{D}_{s\neq I} = \mathrm{UL}_{s\neq i} + \mathrm{N}_{s\neq i},
\end{aligned}$$

and the fractional bound tracer is:

$$\frac{\text{bound tracer}}{\text{total ligand}} = \frac{\mathrm{N}_{s\neq i}}{\mathrm{UL}_{s\neq i} + \mathrm{N}_{s\neq i}}. \tag{3.9}$$

The tracer binding or its displacement with cold isotope will be almost the same based on either Eq. 3.9 or Eq. 3.8.

Plots of the relation in Eq. 3.9 are shown in Fig. 3.12A. Again, for certain values of the initial level of tracer occupancy and of the association constant A_{ss}, of the coupling coefficient c' and for the association constant A_{is}, there is a 'hook' on the binding displacement-curve as the concentration of cold isotope is raised.

For both schemes in Eqs. 3.8 and 3.9 the hook appears around a value of [S] equal $A_s\cdot$[S*], however it disappears at higher doses of S.

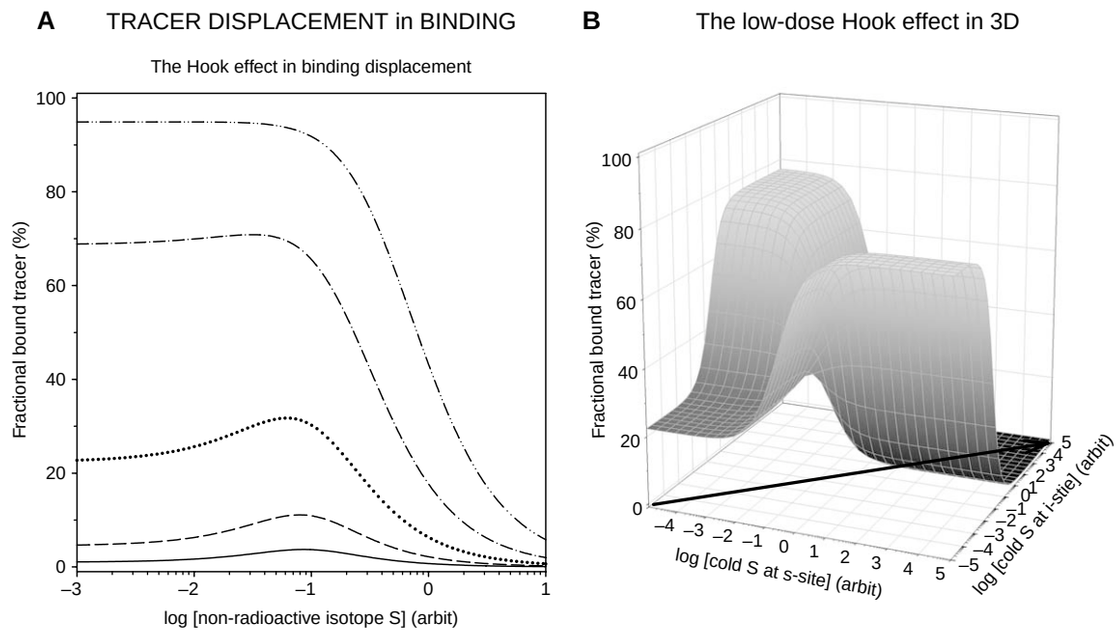

Figure 3.11. Theoretical demonstration of the hook-effect for the two-site one-state model in Fig. 3.10. Association constants A_{ss} and A_{is} are assumed identical. In the 3-D plot tracer concentrations follow the *x*-axis while cold isotope follow the *y*-axis. Parameter c' in 2-D plots varied in 5 steps from 10^{-2} (—) to 10^{2} (– ·· –) by a factor 10.

The plot in 3-D of the low-dose hook effect for $A_{ss} \neq A_{is}$ (Fig. 3.12B) has the same explanation as for the 3-D plot in Fig. 3.11B.

3.4.4. System Constants and the 'Hook'

According to the present 'low-dose hook effect' model, for $A_{ss} = A_{is}$ the hook will appear with increasing concentrations of cold isotope S only when the coupling coefficient starts to increase above a value of circa 10, $c' > 10$, and the product $A_{ss} \cdot S^*$ is less than 1/5, though often clearly visible when the product is 1/10 and below. Absolute requirements for observing the hook are $c' > 1$ and $A_{ss} \cdot S^* < 1$.

For the 'low-dose hook model' with association constants not identical at the two binding sites, i.e., $A_{ss} \neq A_{is}$, the above statements are almost true once the two products $A_{ss} \cdot S^*$ and $A_{is} \cdot S^* < 0.2$.

3.4.5. Initial Occupancy by Tracer, S*

For the two-sited low-dose hook model above, the level of bound radio-activity at low concentration of the displacing ligand S or in its absence is given by inserting zero for [S] in Eq. 3.8, which gives us:

$$\frac{\text{bound radio-actitvity}}{\text{total radio-actitvity}} = \frac{2 \cdot A_{ss} \cdot S^* \cdot (1 + A_{ss} \cdot c' \cdot S^*)}{1 + 2 \cdot A_{ss} \cdot S^* \cdot (1 + A_{ss} \cdot c' \cdot S^*)}, \quad (3.10)$$

for the initial level of occupancy of the tracer when $A_{ss} = A_{is}$.

When $A_{ss} \neq A_{is}$, the initial occupancy by radioactive isotope is given by inserting zero for [S] in Eq. 3.9:

$$\frac{\text{bound radio-actitvity}}{\text{total radio-actitvity}} = \frac{A_{ss} \cdot S^* \cdot (1 + 2 \cdot A_{ss} \cdot c' \cdot S^*)}{1 + A_{ss} \cdot S^* \cdot (1 + 2 \cdot A_{ss} \cdot c' \cdot S^*)}. \quad (3.11)$$

Therefore, in a two-sited receptive system with a large co-lateral intervention coefficient c' equal to strong site interaction, the initial level of bound radio-activity is given by these expressions. The fractional level of bound radio-activity is of interest in RIA assays for two-sited receptive units, as it may be used to choose optimal working conditions (see, e.g., protocols at http://www.gehealthcare.com).

3.4.6. Virtual Observations for A_{ss} and A_{is} and Their Related Sites

As a consequence of the two-sited 'low-dose hook model', there is an astonishing relationship between the two association constants A_{ss} and A_{is} and their pertinent orthosteric and intervention sites, the 's-site' and the 'i-site'. Under the theoretical assumption that the concentration of the cold isotope can change separately at either the s-site or the i-site, i.e., the concentration follows either the *x*-axis or the *y*-axis as indicated in Section 3.4.3 (Figs. 3.11B and 3.12B), there

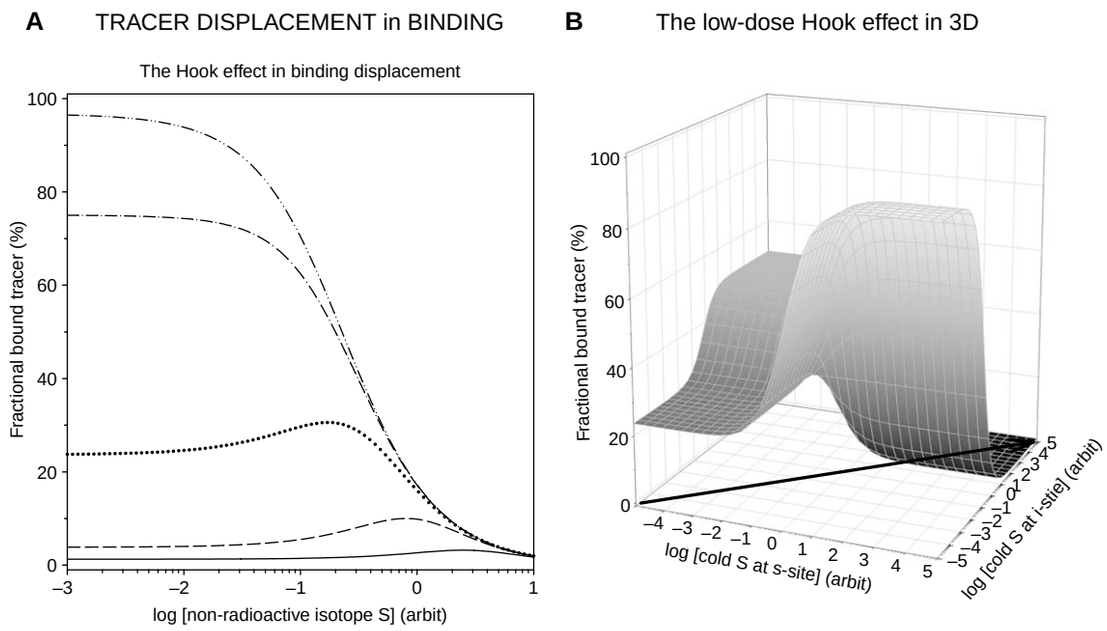

Figure 3.12. Theoretical demonstration of the hook-effect for the two-site one-state model in Fig. 3.10. Association constants A_{ss} and A_{is} are assumed different. In the 3-D plot tracer concentrations follow the *x*-axis while cold isotope follow the *y*-axis. Parameter c' in 2-D plots varied in 5 steps from 10^{-2} (—) to 10^{2} (– ·· –) by a factor 10.

is an unforeseeable consequence. Thus, merely changing S concentration at the s-site (following the *x*-axis), the binding-occupancy profile is solely dependent on the association constant of the other site, A_{is}, and not its own association constant, A_{ss}! This can be seen in Fig. 3.12B. And, vice versa. Only changing S concentration at the i-site (following the *y*-axis), the binding-occupancy curve is solely dependent on the association constant of the opposite site, A_{ss}, and not its own association constant, A_{is}! This is also demonstrated in Fig. 3.12B.

3.4.7. A Non-cyclic Model for Heterologous Intervention

Another model of the intervention scheme is a model in which one of its legs is amputated, as shown in Fig. 3.13. Compare this model with the un-competitive reaction scheme in Chapter 2 (Fig. 2.2D). For convenience, I designate this model the 'non-cyclic model for intervention' (NC-MI). The model is nearly identical to a model by Segel, reproduced in Fig. 2.2C. Segel discussed his model in relation to function. However, we shall look at it as a model for occupancy. Although the NC-MI belong to models with two different ligands in a ternary-complex, and therefore should appear in Chapter 2, I have decided to discuss it here in relation to low-dose hook effects, since the model has been implemented in attempts to explain bell-shaped displacement of bound tracer compounds (Tucek et al. 1990; Proska & Tucek 1994, 1995; Tucek & Proska 1995).

At equilibrium the NC-MI closely resembles the ordinary intervention model. In order to differentiate between the two models, we may write up equations for receptor conformations in both directions of the cyclic scheme and realize that the double set of conformations cancel out and we obtain the equations presented in Chapter 2 (Eqs. 2.16 and 2.17). Conversely, in the NC-MI reaction scheme at equilibrium, the derivations for occupancy are slightly different as the terms for the reaction IR ⇄ IRS are eliminated from the double listing, which result in the following equation for occupancy:

$$\frac{\text{occupancy}}{\text{total}} = \frac{\mathrm{S}/K_{ss}}{\mathrm{S}K_{ss} + \dfrac{2 + \mathrm{I}/K_{ii}}{2 + c \cdot \mathrm{I}/K_{ii}}}. \qquad (3.12)$$

Compare Eq. 3.12 with Eq. 2.16. The effects on occupancy in the NC-MI due to variation in the parameter *c* are illustrated in Fig. 3.14 together with the occupancy variation for the ordinary intervention model; both as a function of the concentration of an interventor.

The difference between the two models is minor. More importantly, the NC-MI at equilibrium cannot explain bell-shaped hook effect behavior by interventor-displacement of occupancy as claimed by Proska and Tucek (1994). The interventor can merely increase or decrease binding of a substrate or an agonist, as demonstrated by Proska and Tucek (1995). Thus, it is unclear to me, which model Proska and Tucek used in their 1994 publication to explain low-dose hook effects in heterologous displacement by alcuronium of [^{3}H]-NMS occupancy at equilibrium (Proska & Tucek 1994, Figs. 5, 6b and 10; Tucek & Proska 1995; Figs. Box 2b and 2).

The NC-MI was also introduced for reverse bell-shaped occupancy found with gallamine on the [^{3}H]-NMS binding in membrane fraction of rat heart atria, although not implemented (Proska & Tucek 1995, Fig. 7).

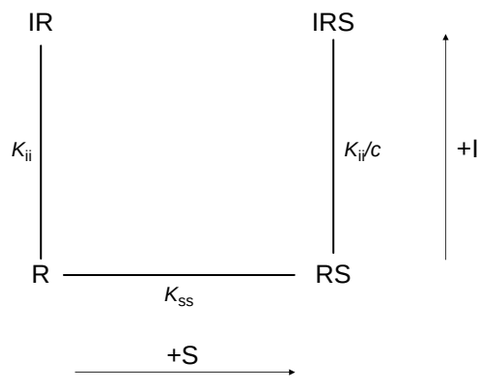

Figure 3.13. A 'non-cyclic model for intervention' (NC-MI). Cutting off the upper leg of the intervention model in Chapter 2 (Fig. 2.1A) results in the NC-MI reaction scheme. Formulation of a distribution equation for this NC-MI reaction scheme is in Eq. 3.12. Compare the NC-MI with a Segel model reproduced in Fig. 2.2C.

3.4.8. Time as an Explanation

More complex models and models involving non-equilibrium schemes have been suggested for the aberrant behavior of heterologous displacement studies demonstrating convex and/or concave bell-shaped concentration-binding relationships (for more details see, e.g., Waelbroeck et al. 1988; Tomlinson & Hnatowich 1988; Marvizon & Baudry 1994; Wreggett & Wells 1995; Lazareno & Birdsall 1995; Ellis 1997; Lazareno et al. 2000; Armstrong & Strange 2001; Neuman-Tancredi et al. 2002; Avlani et al. 2004; Durroux 2005; Franco et al. 2006; Albizu et al. 2006; Fruchart-Gaillard et al. 2006; May et al. 2007).

A play on rate constants as an explanation for the functional substrate inhibition is discussed in more detail for a model in sub-chapter 3.7.

3.4.9. Dynamic Models and Desensitization

To explain non-classical dose-response effects, such as partial agonism and insurmountability, various simple models assuming non-equilibrium conditions have been introduced. In many of these models, desensitization is a through theme. No doubt, on suspicion of non-equilibrium conditions, kinetic (dynamic) models are preferable to all

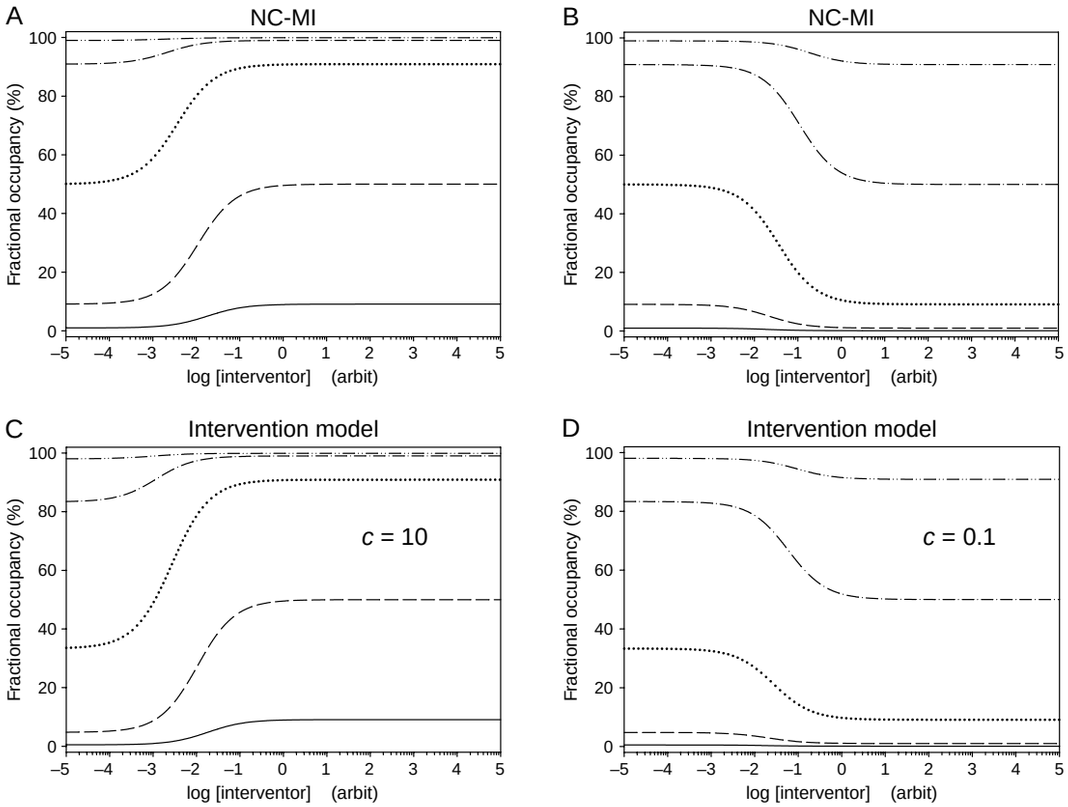

Figure 3.14. Concentration-occupancy relation for the non-cyclic model for intervention (NC-MI; Fig. 3.11), and the intervention model (IM-OSM; Fig. 2.1A). Plots of NC-MI are in panels A and B and plots of IM-OSM are in panels C and D. The heterologous interventor is the independent variable in all plots, while the interaction parameter c is either >1 (panels A and C), or <1 (panels B and D). The fixed substrate or agonist concentration vary between 10^{-1} (—) and 10^{3} (– ·· –) in five steps by a factor 10 with parameters $K_{ss} = 10$ and $K_{ii} = 100$. In both models, the interventor can increase or decrease occupancy of substrate or agonist in a mono-phasic fashion. Bell-shaped or hooked concentration-binding is not possible with these models (see text).

the equilibrium models discussed in this book. However, it is not my intention to analyze dynamic models, therefore, such models should be sought for scrutiny elsewhere in the literature. Examples of dynamic models are Paton (1961), Paton and Rang (1966), Rang (1966), Rang and Ritter (1969), Lüllmann and Ziegler (1973), Gosselin (1977, pp. 325–356), Robertson et al. (1994), Kukkonen et al. (1998), Lew et al. (2000), Vauquelin and Szczuka (2007), and May et al. (2007). A follow-up discussion of the key-paper by Lew et al. (2000) can be found in *Trends Pharmacol Sci* 22; February and July 2001.

3.5. Prelude to Biological Auto-regulation

3.5.1. Self-reference

Self-reference in a general sense is an integral necessity and a prerequisite for regulated and recursive functions of our life and our soul.

Therefore, before I deal with actual examples on hardwired coupling between concentration-dependent auto-regulation and time-dependent auto-inhibition as desensitization, let me briefly introduce some associative aspects related to self-adjustment and homeostatic control in the biosphere together with some substantial examples. Readers who dislike my *bona fide* digressions, can without breaking the continuity skip to the next sub-chapter.

3.5.2. Self-regulatory Mechanisms, Coupled Tightly, Loosely, and in Redundant Parallel

In nature auto-regulatory mechanisms in the biosphere have developed through evolution to a high degree of sophistication. Following less complicated rules, auto-regulatory principles are also found in the non-living nature as 'self-organizing criticality' (e.g., Bak 1997; Jensen 1998; Camazine et al. 2001; Feltz et al. 2006).

Bacteria originated about 1 billion years after the formation of Earth. Notwithstanding, if the intergalactic theory about panspermia (Wickramasinghe 2003, 2005; Hoyle 2005) is correct, creation of auto-poietic (Maturana & Varela 1980) organic life may have taken several billion years to develop instead of just 1 billion years. After

Table 3.2. The development of multicellularity

Epoch of	Ca. years ago $\times 10^9$	References/comments
Earth formation	4.6	Schopf (2002)
Unicellular life as		
Prokaryotes	3.8	
Eukaryotes	3.5	
Multicellular life as		
Homocytics	3.5	
Heterocytics	3.0–2.0	
Early animals	1	Schopf (2002)

Mainly based on Kirk (1998, Chapter 1)

bacteria, just over 2 billion years elapsed to get through unicellular eukaryotes and primitive forms of homo- and hetero-cytics to multicellular organisms (Table 3.2 and Fig. 13.8) (Kirk 1998, Chapter 1; Stephenson et al. 2000; Kessin 2001; Schopf 2002; King 2004; Embley & Martin 2006, Hoenisberg et al. 2008; Abedin & King 2008).

What is organic life? Life is a self-replicating mode based on nucleic acids and on their code; thus including viruses – and may be even smaller entities (Ma & Yu 2006).

Self-reference in auto-poietic or self-replicating organisms is part of organic life, and self-reference expressed in biological activity may be formulated and analyzed in biosemiosis (Hoffmeyer 2008), in memetics, or by functional magnetic resonance imaging (fMRI) (Johnson et al. 2005).

In humanities, in contrast, self-reference and its dominance in intentionality and in the personality appear in signifier-chains of symbolic language without self-reference (Lacan 2007, seminar Feb 18, 1970), in Peirce-related representation (Wenz 2003), also in memetics, and is even afforded by The Providence emerging from 'The mind of God' (Davies 1993).

From a logical point of view, self-reference often ends up in paradoxes (Hofstadter 2007). In the Arts and Letters, covering psycho-analysis, the most elegant paradox in relation to self-reference is the statement 'I lie'. Descartes among others divided the subject of *the subject* into a duality of body-'n-soul. Of course, this view has been disputed repeatedly. The modern understanding of body-'n-soul is a unification of the two, while operating with a divided subject (see, e.g., Lacan 1969; Nordtug 2004; Cavell 2006). Another formulation of the body-'n-soul unification is: ''and the Word (the Father) became Flesh (the Son)''.[2]

Satiety is an example of a mechanism where the description of the coupling between sense, motor-action, and behavior narrows in on the psycho-physical players (Morton et al. 2006). However, I expect that a deeper understanding of the coupling between perception, sense, apperception,[3] affect, intention, and behavior will be debated by our descendants for as long as there are humans around.

3.5.3. Necessary Feed-back or Feed-forward

Initiating a response by an action does not necessarily render an efficient re-action, therefore new recurrent and parallel adjustments are constantly selected to obtain optimal or favorable leverage in living organisms. Design-like, although serendipitous, evolutionary forms of species that have survived depend on smart strategies in all aspects of reproduction. A delicate balance of homeostasis in evo-devo is maintained by regulatory means, such as differential feedback, auto-regulation, and epigenetics (Allis et al. 2007). In addition, coherent control (Shapiro & Brumer 2003; Alon 2006; Palsson 2006) and ordered chaos (Peitgen et al. 1992; Kingsland 1995; Camarzine et al. 2000; Ford 2000, Chapter 12; Turchin 2005, Chapter 5) may begin.

Guiding a single message is often done by parallel, interacting, and self-adjustable pathways in elaborate networks at a molecular scale. Regulated through mechanical or chemical signals and electrical impulses, biological processes have these characteristics. The signal may be a single sub-atomic particle, such as the photon in regulated coherent control of retinal chemistry (Prokhorenko et al. 2006), or atomic scale movements of stereocilia on hair cells in our inner ear (Narayan et al. 1998; Hudspeth 2005). Signaling is sometimes even elicited by quantal release of few molecules (Mallet et al. 2007), although the exact interpretation has been questioned (Ninio 2007). To be sure, quantum mechanics is a base for our understanding of the fabric of the Cosmos (Green 2005) and in the description of coherent control in retinal isomerization. However, quantum mechanics behind our souls has still not reached a trustworthy argumentation for an explanation of our personality. Zohar and Marshall (1990) have argued that human 'self' emerges with Bose-Einstein condensates in our brains. For the single reason that these condensates only exist at extremely low temperatures, the Zohar-Marshall postulates seem to be sheer nonsense.

I believe that the complexity of the human neuronal network at an atomic scale is sufficient for conscious 'self', a so-called apperception (see Section 3.5.2 and footnote 3.3).

3.5.4. Timing by Turn-off

In pathways of biochemical and bio-electrical signal-transduction there are always stringent and severe

[2] '*Homoousion to patri*' ('of one substance with the father'). Council of Nicaea AD 325.

[3] Apperception ∋: human neuronal net's perception of itself as a conscious agent (paraphrased by author).

Figure 3.15. Does the elbow Ache? No, no, no, it displays DYNAMICS. Arm does not hurt – uses acetylcholine-esterase (AChE) to eliminate ACh and perform dynamic and repetitive movements. Drawing by Mette Dreyer (2006). Rights to the figure reside with the author.

turn-off mechanisms, since turn-off is a *sine qua non* for dynamic and repetitive responses. Examples are degradation of acetylcholine by choline esterases at the neuromuscular junction (Fig. 3.15), removal of choline by synaptic re-uptake in a Na and Cl coupled co-transport and of other monoamines (Ribiero et al. 2006; Vialou et al. 2007), decyclization of cyclic nucleotides by phospho-diesterases (Francis et al. 2001), and dephosphorylation of phosphorylated effectors by phosphatases (Forrest et al. 2006).

For the purposeful adaptation of functions, such as the beat of hearts, coordinated visual inputs and outputs, or sudden flight-or-fight reflexes, it has been a prerequisite by haphazard mutation schemes to construct and select feedback and feed-forward regimes with very different dissociation and time constants for turn on-'n-off in most dissimilar environments, in order to create the creatures that have prevailed. Self-control exist widespread in living organisms as feed-back and feed-forward circuits with a span of on-'n-off *time constants* from pico-seconds, to minutes, to days, to years, and even longer and with *dissociation constants* over many orders of magnitude. Photo-isomerization of a retinal chromophore, closure of an ion channel in nerve conduction, beat of hearts, division of a cell, hunger-satiety circles, circadian rhythms, menstrual cycle, hibernation, début of puberty, function of memory and long-term reinforcement and reward mechanisms are examples at either end of our time scale as well as from the middle of it (Table 3.3).

A poignant example of the importance of timing is the function of ion channels orchestrating the heart rhythm in interplay with ion exchangers, pumps, and auxiliary proteins as phopholamban and second messengers. A simple mutation in either a Na^+- or a K^+-channel eliciting an ostensible innocent delay in transport shutting may lead to an early death (Sanguinetti & Tristani-Firouzi 2006; Thomas et al. 2006; Gupta et al. 2007).

3.5.5. Levels of Complexity

On one scale of complexity, we have the classic examples of enzyme feedback control, limiting overgrowth via product and waste material, and enzyme feed-forward substrate inhibition – controlling against metabolic overstimulation (Cornish-Bowden 2004, e.g., Chapter 8),

Table 3.3. Span of time constants by examples from biological functions

Physiological system	Time constant = 1/rate constant	(sec)
Retinal isomerization	Pico- to nanosecond	10^{-9}
Action potential	Millisecond	10^{-3}
Heart beat	Second	10^{0}
Cell cycle	Minute	6×10^{1}
Hunger recursion	Hours	7×10^{3}
Circadian rhythm	Day and night	3×10^{4}
Menstruation	Month	2.6×10^{6}
Hibernation/migration	Months	10^{7}
Lag of puberty	Years	4×10^{8}
Memory	Life time	2×10^{9}

The span of time constants from short to long is a factor of about 10^{20}.

while on other scales of complexity, there is control of seasonal alterations in a single individual of a colony, exemplified by the regulated life cycle of a social slime mold (*Dictyostelium discoideum*) (Stephenson et al. 2000; Bonner 2001; Kessin 2001), control of time for menopause or for parts regulated in Gaia's body (Volk 1997; Lovelock 2000; 2006).[4]

Presentations herein are chiefly drawn from the cellular and sub-cellular level, and will deal mainly with examples of modest complexity, though complex. See, for instance, the description by Agnati et al. (2007) of such complexities by Boolean logic.

In essence, in regulatory systems, the value of TIME CONSTANTS and DISSOCIATION CONSTANTS are keys to optimal function. Features of the time and 'concentration-space' in biology are discussed in sub-chapter 3.6 and presented by examples of time constants in Table 3.3.

3.6. Further Aspects of Auto-regulation and Desensitization

3.6.1. Dose-dependent and Time-dependent Regulation at a Sub-/cellular Level

Responses elicited by agonists in biological systems are often either attenuated or augmented (accelerated) with time, in spite of a maintained and constant stimulatory signal. Langley (1905) described such time-dependent descending responses. The slope of attenuation/acceleration with time may also be dependent on the dose of the agonist. It turns out that lowering of an agonist or metabolite-mediated response, with both time and dose, may involve regulatory knots at a multitude of levels in the signal-transduction chain of events, and these regulatory units can operate by different mechanisms at each level. Behind the nets of knots, the interconnecting regulatory threads have time constants varying from picoseconds to a life span; about 20 orders of magnitude (Table 3.3).

Furthermore, time-dependent fade may require the permanent presence of the eliciting drug, while in other systems, when the stimulatory process is first started, attenuation of a response is by an intrinsic automaticity in the activated molecules. Or, attenuation of the response is incorporated in the function of molecules associated with the signaling pathway, such as auxiliary and scaffolding proteins that can turn the transducing passage on-'n-off (Bhattacharyya et al. 2006; Kolch 2006). Thus, self-regulatory processes are often not dependent on a maintained concentration of an exogenous primary stimulant, not to speak of the stimulants very presence, which might not be needed at all. An example is the spontaneous oscillation in self-sustained Ca^{2+} sensitization underlying Starling's law of the heart. The process includes synchrony of Ca^{2+} channels, Ca^{2+} pumps, Ca^{2+} exchangers, Ca^{2+} buffers, and Ca^{2+} receptors (Armoundas et al. 2007).

3.6.2. The Term Auto-regulation and Possible Derivatives

As mentioned in the Introduction to Chapter 3, 'auto-regulation' in relation to ligand-receptor interactions may cover both ligand-induced alterations in the receptor as well as intrinsic self-control within the receptive unit *per se*. Furthermore, auto-regulation may be CONCENTRATION-dependent and/or TIME-dependent, as will be discussed in the following sections.

In our context of ligand-induced auto-regulation in one-state models, the term is 'auto-intervention' and models for this were presented in sub-chapters 3.1–3.4. In multi-state allosteric auto-regulation, I will use the term concentration-dependent 'auto-modulation' (see Chapters 14 and 15). When there is negative feedback in these situations because of the addition of ligands, the term is 'auto-inhibition' both for CONCENTRATION-dependent auto-regulation and for TIME-dependent desensitization or inactivation. For an overview of the employed terminology, see Table 3.4.

3.6.3. Definitions of Concepts

The above is a rather general introduction to regulation *in time* and *with dose* and needs a couple of examples to illustrate the subject at a cellular or subcellular level. However, to obtain a good overview on the subject of auto-modification for ligand–receptor interactions, it is wise to first realize a few additional concepts and to make these concepts operative through examples.

Thus, I will introduce a simple definition of (a) auto-inhibition, (b) desensitization, and in addition some definitions of (c) related terms (Table 3.4).

Pure auto-ant-agonism[5] appears in steady-state and equilibrium experiments of response versus CONCENTRATION of a ligand as a lower response than the **load**-relation, while pure desensitization shows its many faces as a spontaneous decay of a response with TIME, following immediately after the addition of the drug that elicits the response. After wash-out, a mix of the

[4] Natural self-control in the reproduction of Man is sabotaged by Man. Laws announced in letters of declaration in politics or in the name of God lead indirectly to a malignant overpopulation. Religious and research-based decrees are players in this deregulation – or are they just part of Nature's plan?

[5] Ant-agonism is defined in Chapters 2 and 5, while auto-ant-agonism is concentration-dependent auto-inhibition or concentration-dependent negative auto-modification (Table 3.4).

Table 3.4. Tentative derivatives for the term 'auto-regulation'

Auto-regulation		
Ligand-, voltage- or state-dependent	TIME-dependent **T-dep**	CONCENTRATION-dependent **C-dep**
	Model-**in**dependent	
Ligand-dependent (LGCs, GPCRs, TKRs)	Sensitization	positive auto-modification
	desensitization =	**negative auto-modification** =
	T-dep auto-inhibition	C-dep auto-inhibition also equal to 'auto-ant-agonism'
Voltage-dependent (VOCs)	Sensitization	auto-activation
	Inactivation	**auto-inhibition**
	Model-dependent	
One-state models	**intrinsic** activation/desensitization/ inactivation	positive or negative
	Extrinsic desensitization/inactivation	**auto-intervention**
Two-state or multi-state models	**intrinsic** desensitization/inactivation	positive or negative
	Extrinsic desensitization/inactivation	**auto-modulation**
		in a restricted form it is positive or negative **co-operativity**

'Auto-modification' covers auto-intervention and auto-modulation and may also cover bell-shaped synagics, whereas 'co-operativity' is related solely to steeper (positive) or shallower (negative) slopes of the **load** relationship.
The terms 'intrinsic' and 'extrinsic' seem to refer to 'ligand-independent' and 'ligand-dependent'.
In the table there is no discrimination between models of binding and function.

two, auto-ant-agonism and desensitization, is eventually seen as a reduced response to a second application of the same or another drug.

Desensitization is defined and detailed below and illustrated in Figs. 3.16 and 15.13B, while auto-ant-agonism is shown in Figs. 3.2 and 3.3 and depicted in Fig. 3.16A.

3.6.4. Homologous and Heterologous Desensitization for G protein-coupled receptors (GPCRs)

Here, it suffices to briefly mention the time-dependent desensitization for GPCRs either by the agonist itself, *homologous desensitization*, or alternatively as a reduced response to a given agonist engendered by exposure to agonists of distinct receptor systems, *heterologous desensitization*. In other words, desensitization may be detected as a lowering of the response to a second application of a drug shortly after wash-out of the drug from a first application. In case the drug used is the same in two test additions, lowering of the response in the second application to the drug is named *homologous desensitization* (Fig. 3.16C).

On the other hand, when it is two different agonists used in two test applications, with removal of the first drug in between, showing a lowering in response to the application of a second drug when compared to an earlier control stimulus by this second drug, then the attenuation is said to be due to a '*heterologous desensitization*' (Fig. 3.16C+D) (Lefkowitz et al. 1986; Sibley et al. 1986; Freedman & Lefkowitz 1996; Chuang et al. 1996; Pitcher et al. 1998; Ferguson & Caron 1998; Bunemann & Hosey 1999; Bunemann et al. 2001; Ehlert 2003; Fortin & De Lean 2006; Lefkowitz 2007).

Heterologous desensitization is especially induced by shut-down of the receptor function due to phosphorylation by second-messenger protein kinases, such as PKA and PKC, while the homologous desensitization is also effectuated through phosphorylation by members of the family of G protein-coupled receptor kinases (GRKs), a family consisting of seven subfamilies (Premont et al. 1995; Hisatomi et al. 1998; Weiss et al. 1998; Bunemann & Hosey 1999).

So far, in both writing and in reality, the most decimated mechanisms for homologous and heterologous desensitization seem to be those of serine-/threonine- or tyrosine-phosphorylation/dephosphorylation. The phosphorylation of serine/threonine (S/T) and tyrosine (Y) residues goes through activation of GRKs and second messenger activated kinases, SMPK = PKA and PKC, while signal turn-off is dephosphorylation by S/T- and Y-phosphatases, PP1-2 and PTPs (Shi et al. 1998). In signal-transduction, phospho-relay systems of phosphorylation and dephosphorylation involving basic and acidic amino acid residues as histidine and aspartic acid are more often seen in two-component signaling in prokaryotes (Hoch 2000; Maeda et al. 2006; Szurmant et al. 2007), although also described for eukaryotes (Curien et al. 2007), and sporadically for mammalian systems (Klumpp & Kringlstein 2005).

3.6.5. Intrinsic and Extrinsic Desensitization in Receptive Units Including GPCRs

Rearrangement of intra-molecular residues with intrinsic inactivation mechanisms for voltage-operated channels

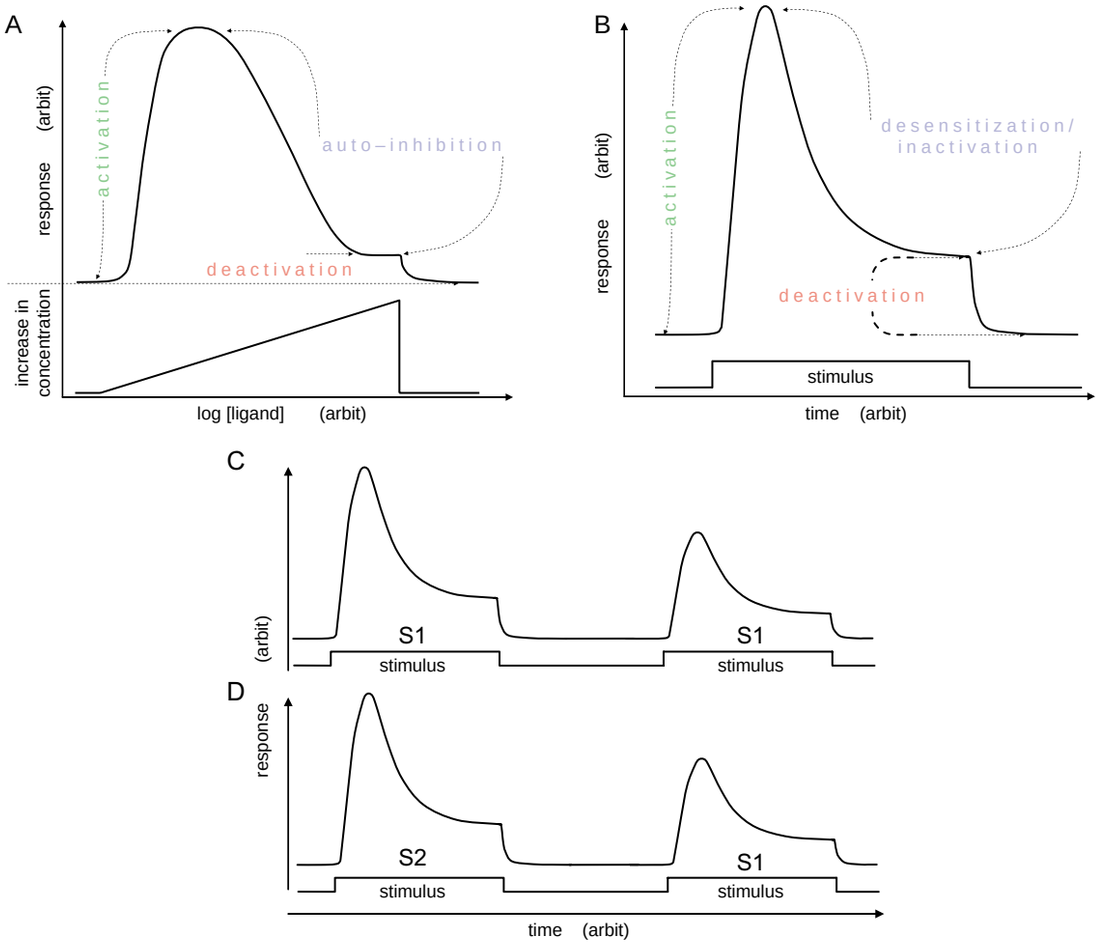

Figure 3.16. Principal diagram of auto-inhibition. Panel A: auto-inhibition due to rising ligand CONCENTRATION. Assuming a one-state reaction scheme it is 'negative auto-intervention', whilst based on a two-state model it is a 'negative auto-modulation'. Panel B: Auto-inhibition as a function of TIME is either a 'desensitization' or an 'inactivation' of the induced activation, some times during a constant stimulus. Panel C: a control response by a ligand S1 is reduced in a second application of the same ligand. This phenomenon is termed 'tachphylaxia' or 'desensitization'. Panel D: a ligand S2 that reduces a control response of a different ligand S1 is characterized as a 'heterologous desensitization'; opposite to the desensitization in panel C that is a 'homologous desensitization'. In general, when a stimulus is removed, there is a 'deactivation' of the response.

(VOCs) (Zagotta et al. 1990) is also seen for intrinsic desensitization in ligand-operated channels (LOCs) (Revah et al. 1991; Devillers-Thiery et al. 1993; Galzi et al. 1996; Mourot et al. 2006a,b). Meanwhile, molecular rearrangements within GPCRs and other desensitizing receptive molecules, such as tyrosine kinase receptors (TKR), are mainly regulated by external modulation with a longer half-time. Altered structural arrangements globally or of specific amino acid segments in G protein-coupled receptor molecules upon activation may induce lowered activity of the receptive unit. Lowered activity by phosphorylation and internalization of the receptive unit is based on G protein-coupled receptor kinases, second messenger kinases, arrestins, SNAREs, and dynamin (DeWire et al. 2007; Lefkowitz 2007; Rizo & Dai 2007; Violin & Lefkowitz 2007). Other means of auto-attenuation or auto-abrogation of the GPCR-signal are by control of the GTPase activity in the related G proteins regulated by 'regulators-of-G protein-signaling' proteins (RGSs) (Dhami & Ferguson 2006). An *intrinsic desensitization* similar to VOC inactivation or intrinsic desensitization of LOCs has still not been described for the GPCRs or TKRs. The intrinsic desensitization is usually a fast process, within milliseconds to seconds (Giniatullin et al. 2005), while the extrinsic desensitization by phosphorylation mechanisms in the GPCRs takes place within minutes, although both sub-minute and hour-long half-times have been reported. As an example, homologous desensitization is often fast with a $t_{1/2} < 20$ s, whereas the heterologous desensitization is a slower process with a $t_{1/2} > 2$ min (Roth et al. 1991).

For many enzymes, and especially for members within the superfamily of kinases, there is self-inhibition due to intra-molecular sequences that are substrate-like (Francis et al. 2002). This mechanism may rather be classified under enzymes with *intrinsic* auto-ant-agonism for activation.

3.6.6. 'Mixed' Auto-inhibition and Desensitization

Desensitization is also a concentration-dependent phenomenon, i.e., the greater the stimulus, the larger the ensuing decay. The higher the concentration of agonists and the more prolonged the stimulus employed in the initial exposure, the more dramatic the reduction in response to a second test solution of an agonist.

Cumulative dose application may yield a dose-response relationship as shown in Fig. 3.17A, where each of the steady-state levels of response may be plotted against the actual agonist concentration (Fig. 3.17B). For this type of cumulative dose-response curve, we could use the term 'concentration-dependent desensitization', but since it would likely confuse some the term is not recommended.

In a narrow sense, the mixed auto-inhibition and desensitization is equal to substrate inhibition, while in a more general sense it may also involve, for example, product inhibition, feedback control through pre-synaptic auto-receptors, removal of the stimulus through degradation or re-uptake of signaling molecules, and phosphorylation by G protein coupled receptor kinases that leads to self-inhibition, through altered GTPase activity induced by RGSs, by guanine nucleotide exchange factors (GEFs), and by GTPase activating proteins (GAPs) or even down-regulation of receptors by internalization (Koenig & Edwardson 1997; Zhang et al. 1999) via endocytosis (Shimada et al. 2007).

You have or will experience that although auto-inhibition has CONCENTRATION of an agonist as its independent variable and desensitization has TIME as its independent variable for a triggered response induced for instance by a fixed agonist concentration, the recording and analysis of these two phenomena are often mixed. Thus, in the practical and daily use of the two terms, they refer in general to an attenuation of a response elicited by a permanently present ligand – a substrate, an agonist, or a transportee. That is what you will be acquainted with. Here, I shall try to keep a clear distinction between concentration-dependent auto-inhibition and time-dependent desensitization, as illustrated in Figs. 3.16 and 3.17 and listed in Table 3.4, in an attempt to analyze the mechanisms underlying self-inhibition by synagic models.

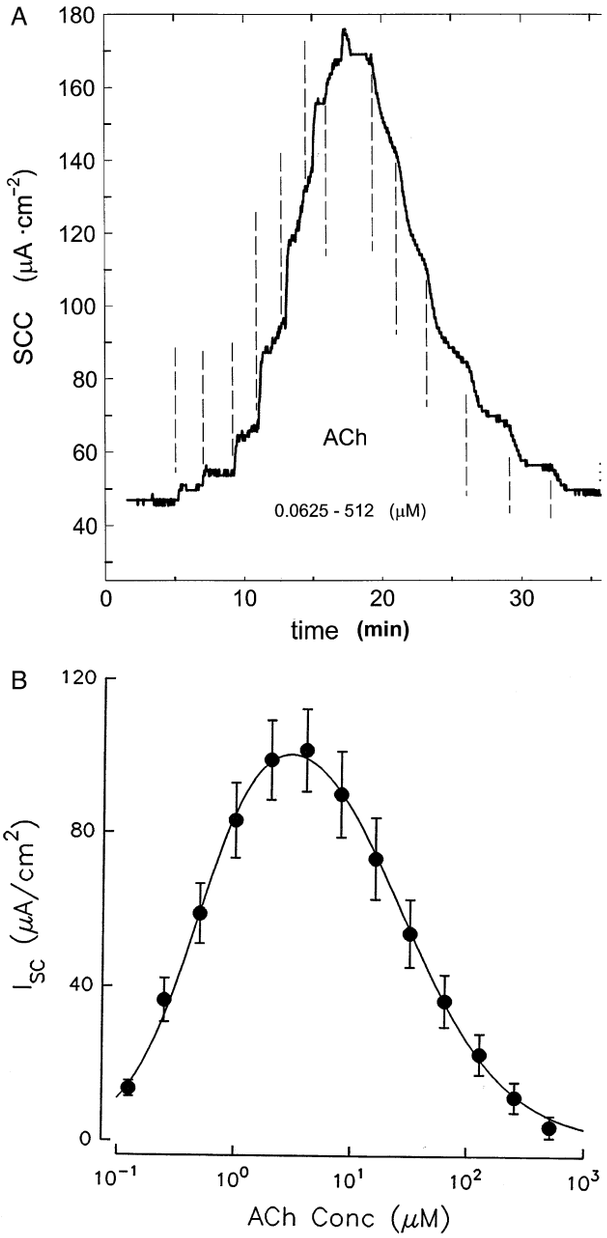

Figure 3.17. A mixture of desensitization and negative auto-modulation. Short circuit current (SCC) induced by acetylcholine in stripped tracheal epithelium from hens. The dose-response curve in panel B is based on data from pseudo-steady-state or equilibrium conditions similar to the induced short circuit current with increasing concentrations of acetylcholine (Ach) in panel A. The time component in A is eliminated in B. Extracting the pure concentration-dependent attenuating effect, auto-inhibition, as shown in Fig. 3.17B, is not an illustration of TIME-dependent desensitization *in sensu strictu*. The 'pure' concentration-dependent attenuating effect in Fig. 3.17B should, therefore, be referred to as concentration-dependent auto-inhibition or auto-ant-agonism. (Courtesy of Dr. B. Winding, unpublished).

Before I continue with examples of desensitization and auto-ant-agonism, it is worth reminding ourselves about definitions of a few other related reactions as illustrated in Fig. 3.16 and presented in Section 3.6.7.

3.6.7. Two-state Models (TSMs), Two-site Models (2SMs) and Auto-inhibition

Two-state models with only one-site (shown in Table 3.5 and described in Chapter 5), belong to the field of intrinsic and TIME-dependent desensitization, while two- (or more) *site* models, including the intervention model described in Chapter 2, more naturally go along with the ideas of CONCENTRATION-dependent auto-inhibition. Thus, strictly speaking, auto-inhibition requires models with at least two binding sites.

A reversible and cyclic model that combines both two states and two sites is described in Chapter 7. This reversible, cyclic TSM may belong to a spontaneous, intrinsic type TIME-desensitization mechanism as well as to an intervention CONCENTRATION-dependent auto-inhibitory mechanism, where the resultant conformational change gives a lower activity at higher concentrations of an interventor or a modulator. Auto-inhibition, contrary to desensitization and heterotropic competitive inhibition type I, still requires an additional binding site, i.e., a receptive unit with a minimum of two sites. Thus, the two-state reaction scheme in its basic form (Fig. 2.1B), with only one binding site, is only relevant for intrinsic desensitization or competitive inhibition type I.

3.6.8. Desensitization and Deactivation

'Deactivation' is the disappearance of a response with time upon removal of a triggering stimulus such as a substrate, an agonist, or a transportee. Thus, deactivation is the reverse mechanism of the activating conformational change, while mechanisms of desensitization for ligand gated channels or mechanisms of inactivation for VOCs result in 'tail' currents that have their base in mechanisms that are separate from the tail currents of deactivating conformational changes.

Desensitization and deactivation are separate phenomena, although they may be interconnected (Barberis et al. 2007). The desensitizing response in channels may be resolved from the process of deactivation, by experimentally determining their individual time constants, i.e. τ_{off} for deactivation from τ_{on} for desensitization. This can be a challenging experiment, when time constants for both activation and desensitization are in the millisecond range. Deactivation and desensitization have been studied in detail in for instance GABA-A receptor-channels (Jones & Westbrook 1995; Barberis et al. 2007). As an example from one such study, the deactivation time constant was determined to be 0.6 ms and the desensitizing time constant resolved was 4 ms for a ligand gated GABA-A channel (Silver et al. 1996).

3.6.9. Desensitization and Gating Currents

Even two humps in I-V diagrams may be due to charge movements in the electrical field across the cell membrane as the gate of VOCs are activated for the channel opening. These charges sit in the fourth TM domain, S4, of cation channels such as the *Shaker* K^+ channel, and the movement of these charges in the electrical field is referred to as gating current. Gating currents for VOC channels have been studied in great detail by Bezanilla, Armstrong, and co-workers as well as by many others (Blunck et al. 2005; Armstrong 2006; Bezanilla 2006; Campos et al. 2007; Savalli et al. 2007). Also 'gating' currents that are found, for instance, in relation to co-transfer of ions and neutral nutrients, may be used for the detailed analysis of transport mechanisms in co-transporters (Eskandria et al. 2005; Loo et al. 2006). However, a prototype cotransporter, such as the sodium/D-glucose transporter (SGLT) (Wright et al. 2007) and the sodium-calcium exchanger (NCX) (Pott et al. 2007) normally do not 'desensitize'.

Finally, the deactivating tail current, as indicated in Fig. 3.16, and overshoot 'tail' current are due to channel and capacitative charge (ion) movements following the opening and closing of channels (Clay 1989; Hong & Wang 2005; Zhang et al. 2005). These two transient currents must be kept separate from accelerated gating and inactivating/desensitizing current changes.

3.6.10. Bell-shaped Dose-response Curves

Auto-inhibition as the concentration of a ligand is raised may display bell-shaped dose-responses as depicted in Fig. 3.16. This regulatory behavior at high agonist or substrate concentration may have different mechanisms.

It may be due to an allosteric site at the receptor itself with a lower affinity for the agonist. Thus, with a negative influence on receptor activity, we may observe either negative co-operativity or a full-blown bell-shaped response. This mechanism is described by the complete intervention model in sub-chapter 3.3 (Eq. 3.5) and relevant for substrate inhibition of enzymes.

Another possibility is a withheld dissociation of GPCRs from the cogent G proteins when agonist-activated. The maintained dissociation is due to a phosphorylation and an association of beta-arrestins at the cytoplasmic loops and tails of GPCRs preventing their re-association to G proteins. The higher the agonist concentration,

Table 3.5. Examples of receptors and effectors as enzymes and transporters in six categories. (For acronyms search in PubMed.)

Category I	ENZYMES	
	ATP-transferases = kinases (see superfamily of kinases)	
	Examples	Second messenger kinases: PKA, PKB, PKC G protein coupled receptor kinases (GRKs) calmodulin kinase II, casein kinase, phosphorylase b kinase
	Phosphohydrolases	
	Examples	Phosphoprotein phosphatases/phosphorylase b PP1 splits covalently bound serine/threonine – phospho-groups PP2A+B splits covalently bound tyrosine – phospho-groups
Category II	TRANSPORTERS	
	Channels	Voltage operated channels (VOCs)
	Examples	(Na^+, K^+, Cl^-, Ca^{2+}) Ligand-gated channels (LGCs or LOCs)
	Examples	(nAChR, iGluRs, 5-HT3, GABAA+C, GlyR, ENaC, CFTR)
	Pumps	
	Examples	V-ATPases (Na,K-ATPase, Ca-ATPase = SERCa or PMCa, H,K-ATPase) F0-Fi ATPase, ABC-transporters, Efflux pumps type I, II, III (Fig. 6.16)
	Co- and counter transporters	
	Examples	NBC, CCC1-5, NIS, NHE, HKE, AE1-5, NCX, NIS Sodium nutrient- and vitamin-coupled: SGLT, NTC, SVCT Na^+-neurotransmitter-coupled: Choline, Serotonin, DOPA, GAT-2
	Uniporters	
	Examples	Gluts, Urea-, Nucleotide-transporters OATs, OATP, DMT, Ferroportin
Category III	RECEPTORS	
	G protein-coupled receptors	GPCRs
	Tyrosin kinase receptors	TKRs receptor and non-receptors
	Examples	Growth factor receptors, hormone receptors, transmitter receptors
Category IV	CARRIERS	
	Extracellular	
	Examples	Hgb, Albumin, TCII, Transferrin TBG, cholesterylester transfer protein CETP
	Intracellular or membrane bound	
	Examples	Mobilferrin, FAPP2 lipid/protein
Category V	OTHER EFFECTORS	
	Motor molecules	
	Examples	Dynamin, actin-myosin, SNAREs°
	Auxilliary molecules	
	Examples	Scaffolds, anchoring, adapters
Category VI	NETWORKS OF EFFECTORS	
	*Iconographical diagrams***	=representing internal structure
	Edge-knot and arrow diagrams	=networks****

°On SNAREs as motors see Rizo and Dai (2007).
**On logical diagrams see, e.g., Vidler (2006, pp. 120–129) and Stjernfelt (2007).
***On networks see chapter 13.

the higher the number of phosphorylated and beta-arrestin-associated GPCRs; locked as non-functional.

A third possibility is a reduction in the GPCRs at the surface of cells due to internalization of activated receptors (Koenig & Edwardson 1997; Zhang et al. 1999; Newman-Tancredi et al. 2002; Shimada et al. 2007). This process is referred to as 'down-regulation' and the removal of the receptors may even include a degradation of the internalized receptors in lysosomes instead of recycling to the cell membrane (Urbe 2005; Zhou et al. 2007). This results in a more permanent auto-inhibition.

As a fourth possibility of bell-shaped dose-response curves, a popular theory is invoked for growth factors and other peptide agonists as well as for antibodies. The model is based on the factual required dimerization for activation of antigen and growth factor receptors in a mono-ligand-dimer-receptor complex. As the concentration of either antibody or peptide ligand rises, chances increase of forming inactive mono-ligand-mono-receptor complexes (Fig. 3.18). This mono-mono complexation at increasing ligand concentrations can explain the decaying leg of observed bell-shaped dose-response curves

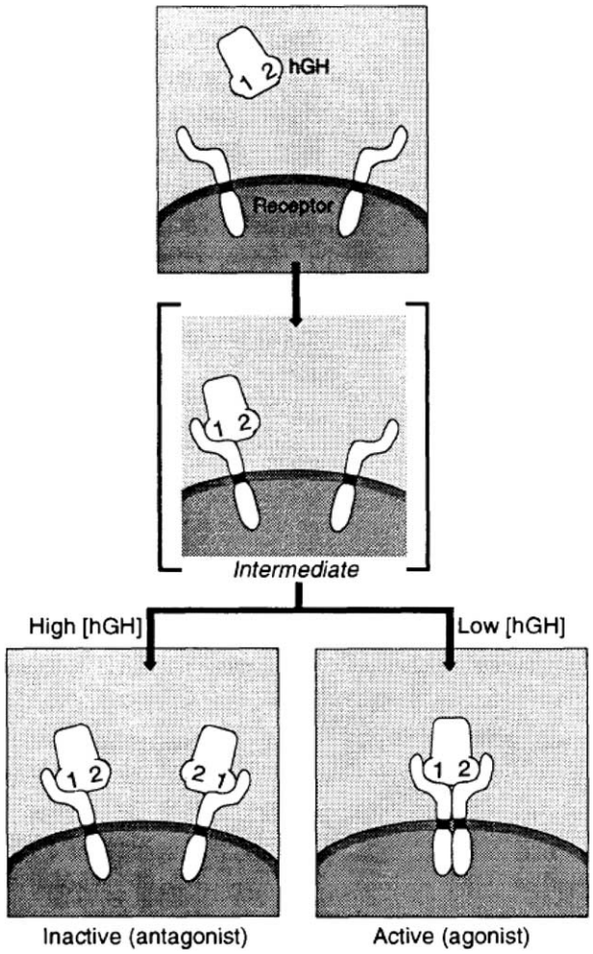

Figure 3.18. A model for bell-shaped synagics in functional dimerization. High dose of human growth factor (hGH) or antibody favors hGH/hGH-receptor or antigen-antibody monomeric complexes and prevents the formation of active dimeric complexes. From Fuh et al. (1992; Fig. 1) with permission.

(Fig. 3.19) (Maeyama et al. 1988; Fuh et al. 1992; Ilondo et al. 1994; de Boer et al. 1996; Urso et al. 2003).

A fifth possibility for upward bell-shaped dose-response curves is negative regulation through auxiliary receptor proteins as the RGSs (Cladman & Chidiac 2002; Dhami & Ferguson 2006).

Finally, downward or reverse bell-shaped dose-responses with an accelerating activity at increasing concentrations of a single ligand are also frequently seen for GPCRs (Accamzzo et al. 2002; Hornigold et al. 2003), and a suggestion for the underlying mechanism was offered by Bindslev (2004).

3.6.11. Constitutive Desensitization

Artificially mutated or 'naturally' mutated G protein coupled receptors may display constitutively desensitized receptor activity, and thus be the cause of illnesses (Pei et al. 1994; Barak et al. 2001, 2003; Rankin et al. 2006). Spontaneously desensitized receptor units are also found for LOCs, as the nicotinic acetylcholine receptor (Changeux & Edelstein 2005, p. 97).

3.6.12. Desensitization-inactivation and the Induction-versus-selection Problem

The conformational induction versus conformational selection problem described in sub-chapter 5.11 is the same for desensitization-inactivation as for activation, except that desensitization-inactivation requires the activation step preceding the inactivation-desensitization step (see Fig. 5.2). Therefore, in essence, inactivation-desensitization is a three-state model. The three states are (1) a reactive state to which agonist can bind,[6] (2) spontaneous or induced conformational flip-flop between a reactive and an active state, which leads to (3) a spontaneous or induced inactivated-desensitized state, by an intrinsic or an extrinsic mechanism (Fig. 5.2).

3.7. Kühl's Minimal Recovery Model for Bell-shaped Synagics

3.7.1. A Recovery Model

Another model for bell-shaped dose-responses in functional studies was formulated by Kühl (1994).

In this book substrate inhibition or auto-inhibition at high ligand concentrations is termed auto-intervention or auto-modulation; conditioned on the selected reaction scheme. Kühl introduced the subject of substrate inhibition with the following statement: ''although recognized early on as an almost universal phenomenon, it has nevertheless met an almost universal disinterest'' and ''Probably the main reason for this neglect is that the majority of enzymologists and many authorities in the field regard substrate inhibition as being almost always a non-physiological phenomenon''.

Besides auto-inhibition, other terms for high substrate inhibition are (1) high-dose inhibition, (2) auto-antagonism, (3) auto-desensitization, (4) self-blockade, (5) excess ligand inhibition, (6) bell-shaped dose-response relationship, and (7) the Arndt-Schulz law. The Arndt-Schulz law is, however, on the sideline. It stems from the homeopathic field – stating that small doses may have a beneficiary effect, while large doses may be self-inhibitory (Clark 1937).

[6] The reactive receptor in itself actually has two conformations or states, an unbound and a bound state, thus adding one more state to the above counting (see Fig 5.2). In reality there are even more states. Observe though, that for modeling of allostery, 'states' are only for un-liganded receptor conformations as defined and described in Chapters 14 and 15.

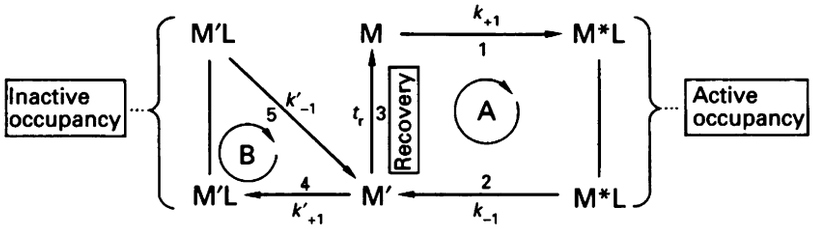

Figure 3.19. Kühl's minimal recovery model. Reproduced from Kühl (1994; Fig. 3) with permission.

Kühl suggests a reaction scheme for auto-inhibition, which he calls 'the recovery model'. This model also suggests new ways to explain such diverse phenomenon as partial agonism, pulse generation, desensitization, memory effects, and ultra-sensitivity.

Certain liganded states are shown twice in Kühl's general reaction scheme in order to emphasize steps in his recovery model. For instance R*S equals both ligand bound and activated, and R′S equals both ligand bound and non-activatable (desensitized) states. Thus, Kühl models deviate on several points from an ordinary reversible kinetic scheme (Kuhl 1994; Kuhl & Jobmann 2006).

3.7.2. Formulation of Kühl's Minimal Recovery Model

Kühl's minimal recovery model is shown in Fig. 3.19.

Direct return from an activated state R*S to a reactive (reactivatable) state R is not possible in Kühl's general model. Thus, $R^* \rightarrow R$, termed deactivation,[7] is not allowed, while recovery in a step from a non-activatable (refractory) state R′ to an activatable (reactive) state R, i.e., $R' \rightarrow R$, is allowed. Further, R* and R*S are lumped together as well as R and RS. Thus, by release from the conventional symbolization, certain elements and pathways are eliminated, and with lumped conformations we reach a rather simple graphical representation, a so-called minimal recovery model (Fig. 3.19).

Notice, in Kühl's minimal recovery model for auto-inhibition even the RS complex is lumped together with the free conformation of the receptor in the resting state, R, and both referred to as R.

Essential features of the minimal recovery model by Kühl are the association of agonist S with R and with R′ having *rates* $k_{+1} \cdot S \cdot R$ and $k'_{+1} \cdot S \cdot R'$, and the dissociation of RS and R′S with the *rate constants* k_{-1} and k'_{-1}. Only the complex R*S is active. The activity is proportional to the concentration of R*S and/or the time spent in this configuration. R is locked in its refractory or non-activatable form R′, when an agonist, S, binds to this isomeric conformation.

[7] Kühl use the term 'deactivation' at variance with its use in this book (see, e.g., Fig. 3.16).

The essence of the minimal recovery model is the balance between the time constant, t_r, for recovery from R' to R and the association constant $k'_{+1}S/k'_{-1}$ for the association with, and dissociation of the agonist from the refractory state of the receptor, R′.

The probability that reaction $R' \rightarrow R$ happens instead of the reaction $R' \rightarrow R'S$ is therefore given by the stochastic frequency that reaction $R' \rightarrow R'S$ does not occur within the fixed recovery time of t_r. The recovery is a waiting process described by a Poissonian distribution

$$P = \exp(-k'_+ \cdot S \cdot t_r), \tag{3.12}$$

and the $R' \rightarrow R$ isomerization has a fixed duration called t_r. The recovery time t_r may be put equal to $1/k_r$, where k_r is the frequency of the recovery, although not a genuine rate constant.

In the formulation of the minimal recovery model, S designates concentration of substrate/agonist S, [S], or concentration of substrate/agonist S normalized by its equilibrium dissociation constant K_s. To simplify the analysis, we assume that $K_s = 1$; thus S is [S] or $[S]/K_s$.

Parameters in Kühl's minimal recovery model are:

$\lambda = S/K_s$, and $S/K_s = S$, since as indicated above K_s is assumed $= 1$.

$$\begin{aligned} F &= k_{+1} \cdot t_r \\ P &= \exp(-F \cdot S) \\ A &= k_{-1}/k_{+1} \cdot k'_{+1}/k'_{-1} = K_d/K'_d \\ B &= k'_{-1}/k_{-1} \\ T &= k_{-1} \cdot t_r \end{aligned}$$

The product of A and B is $A \cdot B = k'_{+1}/k_{+1}$ which we may express as a new constant $= C$.

Kühl's equation A9 for the response of his model then becomes:

$$R = \frac{P \cdot S}{P \cdot (1 + S + S \cdot T) + \dfrac{1 - P}{A \cdot B} \cdot [1 + A \cdot S - (1 + ABTS) \cdot P]}, \tag{3.13}$$

which can be slightly contracted and thus reformulated to:

$$\text{response} = \frac{\text{S}}{\text{S} \cdot \left(1 + P \cdot T + \dfrac{(1-P) \cdot A}{P \cdot C}\right) + 1 + \dfrac{(1-P)^2}{P \cdot C}}. \tag{3.14}$$

Here $1-P$ is the probability of not recovering. Although the Kühl model is hampered by non-reversibility, examples of dose-response relations for the model are shown in Fig. 3.20 with a resumé.

On particular features in his model, Kühl states that the presence of an exponential term introduces an asymmetry into the dose-response curves and can elicit an inhibitory leg of the dose-response curve, which can be very steep; steeper than derived for ordinary reaction schemes with conventional rate constants. This is true as demonstrated in Fig 3.20.

3.7.3. Where Does Kühl's Model Fit In?

Kühl's minimal recovery model only requires that high agonist concentration favors an inactive state of a less active isomer of the receptor or effector molecule in order to simulate bell-shaped synagics. Meanwhile, Kühl's model cannot describe activation of a substrate-induced auto-inhibition state by an interventor of the studied system; as found in several systems and discussed in sub-chapter 7.9.

3.7.4. Conclusions on Kühl's

Kühl's model puts forward a simple model for auto-ant-agonism and desensitization by assuming slow reaction kinetics for certain association and dissociation steps. The model omits a selection of generally accepted molecular conformations. Furthermore, pathways between receptor conformations are banned and most steps are irreversible. Kühl derives a hypothetical probability expression based on the relation between rate constants, rates, and recovery time. The latter appears in the exponential function $P-$ or even as a Poissonian expression, see above.

It is commendable to include rates and rate constants, which for simplicity have been heavily suppressed in this tome. However, in the case of Kühl's model, including rates does not necessarily tangle us out of the snares that hamper insight into synagics and kinetics.

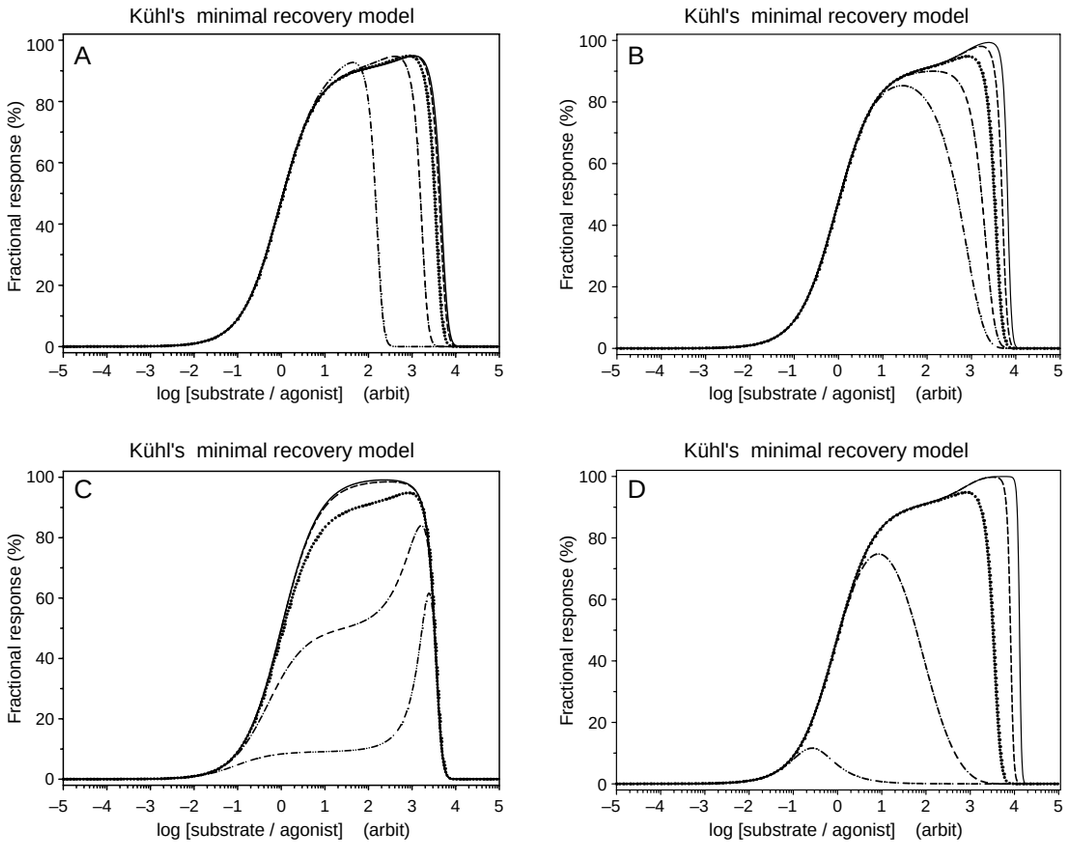

Figure 3.20. Dose-response plots of the Kühl model. Parameters in all plot, when not varied in five steps, were: $F=1.414$, $A=1$, $T=0.1$, and $C=0.01$. (A) Parameter F is varied in five steps from $1.035 \cdot 10^{-3}$ (—) to $3.20 \cdot 10^{-2}$ (– ·· –) by a factor square root of 3. (B) Parameter A is varied in five steps from 10^{-2} (—) to 10^{2} (– ·· –) by a factor 10. (C) Parameter T is varied in five steps from 10^{-3} (—) to 10^{1} (– ·· –) by a factor 10. (D) Parameter C is varied in five steps from 10^{-8} (—) to 10^{4} (– ·· –) by a factor 10^{3}.

Rather, you should start by choosing a fully reversible reaction scheme, as also strongly advocated by Colquhoun (1998). Select the simplest, e.g., the K&T model, and then, as Kühl, add an extra loop with binding of the substrate that somehow inhibits the activated state of the receptor. It may be by binding and conformational change at a secondary site, or as with Kühl, binding of the agonist to a refractory state, and stabilizing that conformation by preventing recovery back to the reactivatable state – the resting state. Study this type of model, even though they do not include *time*, before engaging in non-reversible models. Of course, TIME is a parameter indispensable for the full analysis of kinetics, but its introduction may be postponed until the full implications of synagic analysis are grasped.

Once again, the purpose of this book is to demonstrate that in order to engage in understanding molecular kinetics dependent on time, it is beneficial to start at equilibrium with fully reversible models, before omitting natural pathways and involving more complicated reaction schemes including irreversibility.

REFERENCES

Abedin M & King N. The premetazoan ancestry of cadherins. *Science* 319: 946–948, 2008.

Accomazzo MR, Cattaneo S, Nicosia S & Rovati GE. Bell-shaped curves for prostaglandin-induced modulation of adenylate cyclase: two mutually opposing effects. *Eur J Pharmacol* 454: 107–114, 2002.

Agnati LF, Guidolin D, Leo G & Fuxe K. A Boolean network modelling of receptor mosaics relevance of topology and cooperativity. *J Neural Transm* 114: 77–92, 2007.

Albizu L, Balestre MN, Breton C, Pin JP, Manning M, Mouillac B, et al. Probing the existence of G protein-coupled receptor dimers by positive and negative ligand-dependent cooperative binding. *Mol Pharmacol* 70: 1783–1791, 2006.

Allis CD, Jenuwein T & Reinberg D. *Epigenetics*, 1st ed. Cold Spring Harbor, NY: Cold Spring Harbor Laboratory Press, 2007.

Alon U. *An Introduction to Systems Biology. Design Principles of Biological Circuits*. Boca Raton, Chapman & Hall/CRC, 2006.

Alpers DH. What is new in vitamin B(12)? *Curr Opin Gastroenterol* 21: 183–186, 2005.

Andersen JP, Sorensen TL, Povlsen K & Vilsen B. Importance of transmembrane segment M3 of the sarcoplasmic reticulum Ca^{2+}-ATPase for control of the gateway to the Ca^{2+} sites. *J Biol Chem* 276: 23312–23321, 2001.

Armoundas AA, Rose J, Aggarwal R, Stuyvers BD, O'rourke B, Kass DA, Marban E, Shorofsky SR, Tomaselli GF and William Balke C. Cellular and molecular determinants of altered Ca^{2+} handling in the failing rabbit heart: primary defects in SR Ca^{2+} uptake and release mechanisms. *Am J Physiol Heart Circ Physiol* 292: H1607–H1618, 2007.

Armstrong CM. Na channel inactivation from open and closed states. *Proc Natl Acad Sci USA* 103: 17991–17996, 2006.

Armstrong D & Strange PG. Dopamine D2 receptor dimer formation: evidence from ligand binding. *J Biol Chem* 276: 22621–22629, 2000.

Avlani V, May LT, Sexton PM & Christopoulos A. Application of a kinetic model to the apparently complex behavior of negative and positive allosteric modulators of muscarinic acetylcholine receptors. *J Pharmacol Exp Ther* 308: 1062–1072, 2004.

Bak P. *How Nature Works. The Science of Self-organized Criticality*, 1st ed. Oxford: Oxford University Press, 1997.

Barak LS, Oakley RH, Laporte SA & Caron MG. Constitutive arrestin-mediated desensitization of a human vasopressin receptor mutant associated with nephrogenic diabetes insipidus. *Proc Natl Acad Sci USA* 98: 93–98, 2001.

Barak LS, Wilbanks AM & Caron MG. Constitutive desensitization: a new paradigm for G protein-coupled receptor regulation. *Assay Drug Dev Technol* 1: 339–346, 2003.

Barberis A, Mozrzymas JW, Ortinski PI & Vicini S. Desensitization and binding properties determine distinct alpha1beta2gamma2 and alpha3beta2gamma2 GABA(A) receptor-channel kinetic behavior. *Eur J Neurosci* 25: 2726–2740, 2007.

Berteloot A. Kinetic mechanism of Na+-glucose cotransport through the rabbit intestinal SGLT1 protein. *J Membr Biol* 192: 89–100, 2003.

Bezanilla F. The action potential: from voltage-gated conductances to molecular structures. *Biol Res* 39: 425–435, 2006.

Bhattacharyya RP, Remenyi A, Good MC, Bashor CJ, Falick AM & Lim WA. The Ste5 scaffold allosterically modulates signaling output of the yeast mating pathway. *Science* 311: 822–826, 2006.

Bindslev N. A homotropic two-state model and auto-antagonism. *BMC Pharmacol* 4: 11, 2004.

Blunck R, Chanda B & Bezanilla F. Nano to micro-fluorescence measurements of electric fields in molecules and genetically specified neurons. *J Membr Biol* 208: 91–102, 2005.

Bonner JT. *First Signals: the Evolution of Multicellularity*. Princeton, NJ: Princeton University Press, 2001.

Botts J & Morales M. Analytical description of the effects of modifiers and of enzyme multivalency upon the steady state catalyzed reaction rate. *Trans Faraday Soc* 49: 696–707, 1953.

Bronnikov GE, Zhang SJ, Cannon B & Nedergaard J. A dual component analysis explains the distinctive kinetics of cAMP accumulation in brown adipocytes. *J Biol Chem* 274: 37770–37780, 1999.

Bucher K, Besse CA, Kamau SW, Wunderli-Allenspach H & Kramer SD. Isolated rafts from adriamycin-resistant P388 cells contain functional ATPases and provide an easy test system for P-glycoprotein-related activities. *Pharm Res* 22: 449–457, 2005.

Bunemann M & Hosey MM. G-protein coupled receptor kinases as modulators of G-protein signalling. *J Physiol* 517: 5–23, 1999.

Bunemann M & Hosey MM. Novel signalling events mediated by muscarinic receptor subtypes. *Life Sci* 68: 2525–2533, 2001.

Camazine S, Deneubourg J-L, Franks NR, Sneyd J, Theraulaz G & Bonabeau E. *Self-organization in Biological Systems*, 1st ed. Princeton, NJ: Princeton University Press, 2001.

Campos FV, Chanda B, Roux B & Bezanilla F. Two atomic constraints unambiguously position the S4 segment relative to S1 and S2 segments in the closed state of Shaker K channel. *Proc Natl Acad Sci USA* 130: 257–268, 2007.

Cavell S. *The Claim of Reason: Wittgenstein, Skepticism, Morality, and Tragedy*, New ed. Oxford: Oxford University Press, 1999.

Changeux J-P & Edelstein SJ. *Nicotinic Acetylcholine Receptors: from Molecular Biology to Cognition*, English ed. Baltimore: Johns Hopkins University Press, 2005.

Chuang TT, Iacovelli L, Sallese M & De Blasi A. G protein-coupled receptors: heterologous regulation of homologous desensitization and its implications. *Trends Pharmacol Sci* 17: 416–421, 1996.

Cladman W & Chidiac P. Characterization and comparison of RGS2 and RGS4 as GTPase-activating proteins for m2 muscarinic receptor-stimulated G(i). *Mol Pharmacol* 62: 654–659, 2002.

Clark AJ. *General Pharmacology*, Vol. 4, 1st ed. Berlin: Springer, 1937.

Clark RW. *J.B.S. The Life and Work of J.B.S. Haldane*. London: Hodder & Stoughton, 1968.

Clay JR. Slow inactivation and reactivation of the K+ channel in squid axons. A tail current analysis. *Biophys J* 55: 407–414, 1989.

Colquhoun D. Binding, gating, affinity and efficacy: the interpretation of structure-activity relationships for agonists and of the effects of mutating receptors. *Br J Pharmacol* 125: 924–947, 1998.

Colquhoun D, Dowsland KA, Beato M and Plested AJ. How to impose microscopic reversibility in complex reaction mechanisms. *Biophys J* 86: 3510–3518, 2004.

Cornish-Bowden A. *The Pursuit of Perfection. Aspects of Biochemical Evolution*, 1st ed. Oxford: Oxford University Press, 2004.

Curien G, Laurencin M, Robert-Genthon M & Dumas R. Allosteric monofunctional aspartate kinases from Arabidopsis. *FEBS J* 274: 164–176, 2007.

Davies P. *The Mind of God. Science and the Search for Ultimate Meaning*, 1st ed. London: Penguin Books, 1993.

De Boer RJ, Boerlijst MC, Sulzer B & Perelson AS. A new bell-shaped function for idiotypic interactions based on cross-linking. *Bull Math Biol* 58: 285–312, 1996.

Devillers-Thiery A, Galzi JL, Eisele JL, Bertrand S, Bertrand D & Changeux JP. Functional architecture of the nicotinic acetylcholine receptor: a prototype of ligand-gated ion channels. *J Membr Biol* 136: 97–112, 1993.

DeWire SM, Ahn S, Lefkowitz RJ & Shenoy SK. Beta-arrestins and cell signaling. *Annu Rev Physiol* 69: 483–510, 2007.

Dhami GK & Ferguson SS. Regulation of metabotropic glutamate receptor signaling, desensitization and endocytosis. *Pharmacol Ther* 111: 260–267, 2006.

Durroux T. Principles: a model for the allosteric interactions between ligand binding sites within a dimeric GPCR. *Trends Pharmacol Sci* 26: 376–384, 2005.

Ehlert FJ. Contractile role of M2 and M3 muscarinic receptors in gastrointestinal, airway and urinary bladder smooth muscle. *Life Sci* 74: 355–366, 2003.

Einholm AP, Andersen JP & Vilsen B. Importance of Leu99 in transmembrane segment M1 of the Na+, K+-ATPase in the binding and occlusion of K+. *J Biol Chem* 282: 23854–23866, 2007.

Ellis J. Allosteric binding sites on muscarinic receptors. *Drug Dev Res* 40: 193–204, 1997.

Embley TM & Martin W. Eukaryotic evolution, changes and challenges. *Nature* 440: 623–630, 2006.

Eskandari S, Wright EM & Loo DD. Kinetics of the reverse mode of the Na+/glucose cotransporter. *J Membr Biol* 204: 23–32, 2005.

Feltz B, Crommelinck M & Goujon P. *Self-organization and Emergence in Life Sciences*, 1st ed. Dordrecht: Springer, 2006.

Ferguson SS & Caron MG. G protein-coupled receptor adaptation mechanisms. *Semin Cell Dev Biol* 9: 119–127, 1998.

Ford ED. *Scientific Method for Ecological Research*. Cambridge: Cambridge University Press, 2000.

Forrest AR, Taylor DF, Fink JL, Gongora MM, Flegg C, Teasdale RD, Suzuki H, Kanamori M, Kai C, Hayashizaki Y & Grimmond SM. PhosphoregDB: the tissue and sub-cellular distribution of mammalian protein kinases and phosphatases. *BMC Bioinformatics* 7: 82, 2006.

Fortin Y & De Lean A. Role of cyclic GMP and calcineurin in homologous and heterologous desensitization of natriuretic peptide receptor-A. *Can J Physiol Pharmacol* 84: 539–546, 2006.

Francis SH, Turko IV & Corbin JD. Cyclic nucleotide phosphodiesterases: relating structure and function. *Prog Nucleic Acid Res Mol Biol* 65: 1–52, 2001.

Francis SH, Poteet-Smith C, Busch JL, Richie-Jannetta R & Corbin JD. Mechanisms of autoinhibition in cyclic nucleotide-dependent protein kinases. *Front Biosci* 7: 580–592, 2002.

Franco R, Casado V, Mallol J, Ferrada C, Ferre S, Fuxe K, Cortes A, Ciruela F, Lluis C & Canela EI. The two-state dimer receptor model: a general model for receptor dimers. *Mol Pharmacol* 69: 1905–1912, 2006.

Freedman NJ & Lefkowitz RJ. Desensitization of G protein-coupled receptors. *Recent Prog Horm Res* 51: 319–351, 1996.

Fruchart-Gaillard C, Mourier G, Marquer C & Menez A. Identification of various allosteric interaction sites on M_1 muscarinic receptor using ^{125}I-met35-oxidized muscarinic toxin 7. *Mol Pharmacol* 69: 1641–1651, 2006.

Fuh G, Cunningham BC, Fukunaga R, Nagata S, Goeddel DV & Wells JA. Rational design of potent antagonists to the human growth hormone receptor. *Science* 256: 1677–1680, 1992.

Galzi JL, Edelstein SJ & Changeux J. The multiple phenotypes of allosteric receptor mutants. *Proc Natl Acad Sci USA* 93: 1853–1858, 1996.

Giniatullin R, Nistri A & Yakel JL. Desensitization of nicotinic ACh receptors: shaping cholinergic signaling. *Trends Neurosci* 28: 371–378, 2005.

Gosselin RE. Drug-receptor interaction: a new kinetic model. In: *Kinetics of Drug Action*, 1st ed, edited by van Rossum JM. Berlin: Springer Verlag, 1977.

Green B. *The Fabric of the Cosmos. Space, Time, and the Texture of Reality*, First Vintage Books edition. New York: Vintage Books, 2005.

Griffin MT, Hsu JC, Shehnaz D & Ehlert FJ. Comparison of the pharmacological antagonism of M2 and M3 muscarinic receptors expressed in isolation and in combination. *Biochem Pharmacol* 65: 1227–1241, 2003.

Gupta A, Lawrence AT, Krishnan K, Kavinsky CJ & Trohman RG. Current concepts in the mechanisms and management of drug-induced QT prolongation and torsade de pointes. *Am Heart J* 153: 891–899, 2007.

Haldane JBS. *Enzymes*, 1st ed. London: Longmans, Green & Co, 1930.

Hapfelmeier G, Tredt C, Haseneder R, Zieglgansberger W, Eisensamer B, Rupprecht R & Rammes G. Co-expression of the 5-HT3B serotonin receptor subunit alters the biophysics of the 5-HT3 receptor. *Biophys J* 84: 1720–1733, 2003.

Harper ET. Kinetics of the two-sited enzyme. I. Activation and inhibition by substrate. *J Theor Biol* 32: 405–414, 1971.

Hayashi I, Plevin MJ & Ikura M. CLIP170 autoinhibition mimics intermolecular interactions with p150(Glued) or EB1. *Nat Struct Mol Biol* 14: 980–981, 2007.

Hisatomi O, Matsuda S, Satoh T, Kotaka S, Imanishi Y & Tokunaga F. A novel subtype of G-protein-coupled receptor kinase, GRK7, in teleost cone photoreceptors. *FEBS Lett* 424:159–164, 1998.

Hoch JA. Two-component and phosphorelay signal transduction. *Curr Opin Microbiol* 3: 165–170, 2000.

Hoenisberg HF, Tijaro MH & Sanabria C. From unicellularity to multicellularity – molecular speculations about early animal evolution. *Genet Mol Res* 7: 50–59, 2008.

Hofstadter D. *I Am a Strange Loop*, 1st ed. New York: Basic Books, 2007.

Hong Z, Wang DS. Potentiation, activation and blockade of GABAA receptors by etomidate in the rat sacral dorsal commissural neurons. *Neuroscience* 132: 1045–1053, 2005.

Hornigold DC, Mistry R, Raymond PD, Blank JL & Challiss RA. Evidence for cross-talk between M2 and M3 muscarinic acetylcholine receptors in the regulation of second messenger and extracellular signal-regulated kinase signalling pathways in Chinese hamster ovary cells. *Br J Pharmacol* 138: 1340–1350, 2003.

Hoyle F. *Of Men and Galaxies*. Amhent, Prometheus Books, 2005.

Hudspeth AJ. How the ear's works work: mechanoelectrical transduction and amplification by hair cells. *C R Biol* 328: 155–162, 2005.

Ilondo MM, Damholt AB, Cunningham BA, Wells JA, De Meyts P & Shymko RM. Receptor dimerization determines the effects of growth hormone in primary rat adipocytes and cultured human IM-9 lymphocytes. *Endocrinology* 134: 2397–2403, 1994.

Jarv J, Toomela T & Karelson E. Dual effect of carbachol on the muscarinic receptor. *Biochem Mol Biol Int* 30: 649–654, 1993.

Jensen HJ. *Self-Organized Criticality: Emergent Complex Behavior in Physical and Biological Systems*, 1st ed. Cambridge, Cambridge University Press 1998.

Johnson SC, Schmitz TW, Kawahara-Baccus TN, Rowley HA, Alexander AL, Lee J & Davidson RJ. The cerebral response during subjective choice with and without self-reference. *J Cogn Neurosci* 17: 1897–1906, 2005.

Jones MV & Westbrook GL. Desensitized states prolong GABAA channel responses to brief agonist pulses. *Neuron* 15: 181–191, 1995.

Jow B & Numann R. The effects of ZD6169 on the ATP-dependent K(+) current (I(K)(ATP)) in isolated cat ventricular myocytes. *Eur J Pharmacol* 383: 197–202, 1999.

Kaiser PM. Substrate inhibition as a problem of non-linear steady state kinetics with monomeric enzymes. *J Mol Catal* 8: 431–442, 1980.

Kessin RH. *Dictyostelium: Evolution, Cell Biology, and the Development of Multicellularity*, 1st ed. Cambridge: Cambridge University Press, 2001.

King N. The unicellular ancestry of animal development. *Dev Cell* 7: 313–325, 2004.

Kingsland SE. *Modeling Nature. Episodes in the History of Population Ecology*, 2nd ed. Chicago, IL: The University of Chicago Press, 1995.

Kirk D. *Volvox. Molecular-genetic Origins of Multicalluarity and Cellular Differentiation*, 1st ed. Cambridge: Cambridge University Press, 1998.

Klumpp S & Krieglstein J. Reversible phosphorylation of histidine residues in vertebrate proteins. *Biochim Biophys Acta* 1754: 291–295, 2005.

Koenig JA & Edwardson JM. Endocytosis and recycling of G protein-coupled receptors. *Trends Pharmacol Sci* 18: 276–287, 1997.

Kolch W. Coordinating ERK/MAPK signalling through scaffolds and inhibitors. *Nat Rev Mol Cell Biol* 6: 827–837, 2006.

Kukkonen JP, Näsman J, Rinken A, Dementjev A & Akerman KE. Pseudo-noncompetitive antagonism of M1, M3, and M5 muscarinic receptor-mediated Ca2+ mobilization by muscarinic antagonists. *Biochem Biophys Res Commun* 243: 41–46, 1998.

Kühl PW. Excess-substrate inhibition in enzymology and high-dose inhibition in pharmacology: a reinterpretation. *Biochem J* 298: 171–180, 1994.

Kühl PW & Jobmann M. Receptor-agonist interactions in service – theoretic perspective, effects of molecular timing on the shape of dose-response curves. *J Recept Signal Transduct Res* 26: 1–34, 2006.

Lacan J. *The Seminar of Jacques Lacan. Book XVII. The Reverse Side of Psychoanalysis* (1969–1970), English translation by R. Grigg. New York: WW Norton, 2007.

Laidler KJ. General steady-state equations in enzyme and other catalyzed reactions. *Trans Faraday Soc* 52: 1374–1382, 1956.

Laidler KJ. *The Chemical Kinetics of Enzyme Action*, 1st ed. London: Oxford University Press, 1958.

Laidler KJ & Hoare JP. The molecular kinetics of the urea-urease system. I. The kinetic laws. *J Am Chem Soc* 71: 2699–2702, 1949.

Langley NJ. On the reaction of cells and of nerve-endings to certain poisons, chiefly as regards the reaction of striated muscle to nicotine and to curari. *J Physiol* 33: 374–413, 1905.

Lazareno S & Birdsall NJ. Detection, quantitation, and verification of allosteric interactions of agents with labeled and unlabeled ligands at G protein-coupled receptors: interactions of strychnine and acetylcholine at muscarinic receptors. *Mol Pharmacol* 48: 362–378, 1995.

Lazareno S, Popham A & Birdsall NJ. Allosteric interactions of staurosporine and other indolocarbazoles with *N*-[methyl-^{3}H]scopolamine and acetylcholine at muscarinic receptor subtypes: identification of a second allosteric site. *Mol Pharmacol* 58: 194–207, 2000.

Leboeuf R, Langlois MF, Martin M, Ahnadi CE & Fink GD. 'Hook effect' in calcitonin immunoradiometric assay in patients with metastatic medullary thyroid carcinoma: case report and review of the literature. *J Clin Endocrinol Metab* 91: 361–364, 2006.

Lefkowitz RJ. Seven transmembrane receptors: something old, something new. *Acta Physiol* (Oxf) 190: 9–19, 2007.

Lefkowitz RJ, Benovic JL, Kobilka B & Caron MG. Beta-adrenegic receptors and rhodopsin: shedding new light on an old subject. *Trends Pharmacol Sci* 7: 444–448, 1986.

Lew MJ, Ziogas J & Christopoulos A. Dynamic mechanisms of non-classical antagonism by competitive AT(1) receptor antagonists. *Trends Pharmacol Sci* 21: 376–381, 2000.

Lineweaver H & Burk D. The determination of enzyme dissociation constants. *J Am Chem Soc* 56: 658–666, 1934.

Loo DD, Hirayama BA, Karakossian MH, Meinild AK & Wright EM. Conformational dynamics of hSGLT1 during Na+/glucose cotransport. *J Gen Physiol* 128: 701–720, 2006.

Lovelock J. *Gaia: a New Look at Life on Earth*. Oxford: Oxford Paperbacks, 2000.

Lovelock J. *The Revenge of Gaia: Why the Earth Is Fighting Back – and How We Can Still Save Humanity*, 1st ed. London: Allen Lane, 2006.

Lüllmann H & Ziegler A. A transient state concept of drug receptor interaction. *Naunyn Schmiedebergs Arch Pharmacol* 280: 1–21, 1973.

Ma W & Yu C. Intramolecular RNA replicase: possibly the first self-replicating molecule in the RNA world. *Orig Life Evol Biosph* 36: 413–420, 2006.

Maeda S, Sugita C, Sugita M & Omata T. A new class of signal transducer in His-Asp phosphorelay systems. *J Biol Chem* 281: 37868–37876, 2006.

Maeyama K, Hohman RJ, Ali H, Cunha-Melo JR & Beaven MA. Assessment of IgE-receptor function through measurement of hydrolysis of membrane inositol phospholipids. New insights on the phenomena of biphasic antigen concentration-response curves and desensitization. *J Immunol* 140: 3919–3927, 1988.

Mallet A, Faber DS & Korn H. Statistical analysis of visual fits: answer to J. Ninio. *J Neurophysiol* 98: 1836–1840, 2007.

Marvizon JC & Baudry M. Allosteric interactions and modulator requirement for NMDA receptor function. *Eur J Pharmacol* 269: 165–175, 1994.

Matsukura S, West CD, Ichikawa Y, Jubiz W, Harada G & Tyler FH. A new phenomenon of usefulness in the radioimmunoassay of plasma adrenocorticotropic hormone. *J Lab Clin Med* 77: 490–500, 1971.

Maturana HR & Varela FJ. *Autopoiesis and Cognition: the Realization of the Living*, 1st ed. Dordrecht: Reidel Publishing Co., 1980.

May LT, Avlani VA, Langmead CJ, Herdon HJ, Wood MJ, Sexton PM & Christopoulos A. Structure-function studies of allosteric agonism at M2 muscarinic acetylcholine receptors. *Mol Pharmacol* 72: 463–476, 2007.

Miles LE. Properties, variants, and applications of the immunoradiometric assay method. *Ric Clin Lab* 5: 59–72, 1975.

Miles LE, Lipschitz DA, Bieber CP & Cook JD. Measurement of serum ferritin by a 2-site immunoradiometric assay. *Anal Biochem* 61: 209–224, 1974.

Monod J, Changeux JP & Jacob F. Allosteric proteins and cellular control systems. *J Mol Biol* 6: 306–329, 1963.

Morton GJ, Cummings DE, Baskin DG, Barsh GS & Schwartz MW. Central nervous system control of food intake and body weight. *Nature* 443: 289–295, 2006a.

Mourot A, Rodrigo J, Kotzyba-Hibert F, Bertrand S, Bertrand D & Goeldner M. Probing the reorganization of the nicotinic acetylcholine receptor during desensitization by time-resolved covalent labeling using [3H]AC5, a photoactivatable agonist. *Mol Pharmacol* 69: 452–461, 2006b.

Mourot A, Rodrigo J, Bertrand S, Bertrand D, Goeldner M & Kotzyba-Hibert F. Reorganization of the nicotinic acetylcholine receptor

during desensitization probed with a photoactivatable agonist. *J Mol Neurosci* 30: 13–14, 2006.

Murayama T, Oba T, Katayama E, Oyamada H, Oguchi K, Kobayashi M, Otsuka K & Ogawa Y. Further characterization of the type 3 ryanodine receptor (RyR3) purified from rabbit diaphragm. *J Biol Chem* 274: 17297–17308, 1999.

Narayan SS, Temchin AN, Recio A & Ruggero MA. Frequency tuning of basilar membrane and auditory nerve fibers in the same cochleae. *Science* 282: 1882–1884, 1998.

Nayyar SN & Glick D. Effect of alcohols on beta-glucuronidase activity. *J Biol Chem* 222: 73–83, 1956.

Newman-Tancredi A, Cussac D, Marini L & Millan MJ. Antibody capture assay reveals bell-shaped concentration-response isotherms for h5-HT(1A) receptor-mediated Galpha(i3) activation: conformational selection by high-efficacy agonists, and relationship to trafficking of receptor signaling. *Mol Pharmacol* 62: 590–601, 2002.

Ninio J. Doubts about quantal analysis. *J Neurophysiol* 98: 1827–1835, 2007.

Nordtug B. Subjectivity as an unlimited semiosis: Lacan and Peirce. *Studies Phil Edu* 23: 87–102, 2004.

Onali P, Adem A, Karlsson E & Olianas MC. The pharmacological action of MT-7. *Life Sci* 76: 1547–1552, 2005.

Palsson BØ. *Systems Biology. Properties of Reconstructed Networks*, 1st ed. Cambridge: Cambridge University Press, 2006.

Paton WD & Rang HP. The uptake of atropine and related drugs by intestinal smooth muscle of the guinea-pig in relation to acetylcholine receptors. *Proc R Soc Lond B Biol Sci* 163: 1–44, 1965.

Paton WDM. A theory of drug action based on the rate of drug/receptor combination. *Proc R Soc Lond B* 154: 21–69, 1961.

Pei G, Samama P, Lohse M, Wang M, Codina J & Lefkowitz RJ. A constitutively active mutant beta 2-adrenergic receptor is constitutively desensitized and phosphorylated. *Proc Natl Acad Sci USA* 91: 2699–2702, 1994.

Peitgen H-O, Jürgens H & Saupe D. *Classical Fractals and Self-Similarity, Chaos and Fractals: New Frontiers of Science*, 1st ed. Berlin: Springer-Verlag, 1992.

Pitcher JA, Freedman NJ & Lefkowitz RJ. G protein-coupled receptor kinases. *Annu Rev Biochem* 67: 653–692, 1998.

Pott C, Goldhaber JI & Philipson KD. Homozygous overexpression of the Na+−Ca2+ exchanger in mice: evidence for increased transsarcolemmal Ca2+ fluxes. *Ann N Y Acad Sci* 1099: 310–314, 2007.

Premont RT, Inglese J & Lefkowitz RJ. Protein kinases that phosphorylate activated G protein-coupled receptors. *FASEB J* 9: 175–182, 1995.

Prokhorenko VI, Nagy AM, Waschuk SA, Brown LS, Birge RR & Miller RJ. Coherent control of retinal isomerization in bacteriorhodopsin. *Science* 313: 1257–1261, 2006.

Proska J & Tucek S. Mechanisms of steric and cooperative actions of alcuronium on cardiac muscarinic acetylcholine receptors. *Mol Pharmacol* 45: 709–717, 1994.

Proska J & Tucek S. Competition between positive and negative allosteric effectors on muscarinic receptors. *Mol Pharmacol* 48: 696–702, 1995.

Rang HP. The kinetics of action of acetylcholine antagonists in smooth muscle. *Proc R Soc Lond B Biol Sci* 164: 488–510, 1966.

Rang HP & Ritter JM. On the mechanism of desensitization at cholinergic receptors. *Mol Pharmacol* 6: 357–382, 1970.

Rankin ML, Marinec PS, Cabrera DM, Wang Z, Jose PA & Sibley DR. The D1 dopamine receptor is constitutively phosphorylated by G protein-coupled receptor kinase 4. *Mol Pharmacol* 69: 759–769, 2006.

Revah F, Bertrand D, Galzi JL, Devillers-Thiery A, Mulle C, Hussy N, Bertrand S, Ballivet M & Changeux JP. Mutations in the channel domain alter desensitization of a neuronal nicotinic receptor. *Nature* 353: 846–849, 1991.

Ribeiro FM, Black SA, Prado VF, Rylett RJ, Ferguson SS & Prado MA. The 'ins' and 'outs' of the high-affinity choline transporter CHT1. *J Neurochem* 97: 1–12, 2006.

Rizo J & Dai H. How much can SNAREs flex their muscles? *Nat Struct Mol Biol* 14: 880–882, 2007.

Robertson MJ, Wragg A & Clark KL. Modulation of tachyphylaxis to angiotensin II in rabbit isolated aorta by the angiotensin AT1 receptor antagonist, losartan. *Regul Pept* 50: 137–145, 1994.

Rodbard D. Radioimmunoassays and 2-site immunoradiometric 'sandwich' assays: basic principles. *Radioisotopes* 37: 590–594, 1988.

Roth NS, Campbell PT, Caron MG, Lefkowitz RJ & Lohse MJ. Comparative rates of desensitization of beta-adrenergic receptors by the beta-adrenergic receptor kinase and the cyclic AMP-dependent protein kinase. *Proc Natl Acad Sci USA* 88: 6201–6204, 1991.

Rovati GE & Nicosia S. Lower efficacy: interaction with an inhibitory receptor or partial agonism? *Trends Pharmacol Sci* 15: 140–144, 1994.

Sanguinetti MC & Tristani-Firouzi M. hERG potassium channels and cardiac arrhythmia. *Nature* 440: 463–469, 2006.

Savalli N, Kondratiev A, de Quintana SB, Toro L & Olcese R. Modes of operation of the BKCa channel beta2 subunit. *J Gen Physiol* 130: 117–131, 2007.

Schlee S, Carmillo P & Whitty A. Quantitative analysis of the activation mechanism of the multicomponent growth-factor receptor Ret. *Nat Chem Biol* 2: 636–644, 2006.

Schopf JW. *Life's Origin: the Beginnings of Biological Evolution*, 1st ed. Berkeley, CA: University of California Press, 2002.

Segel IH. *Enzyme Kinetics. Behavior and Analysis of Rapid Equilibrium and Steady-State Enzyme Systems*. New York: Wiley & Sons (reissued 1993), 1975.

Segal HL, Kachmar JF & Boyer PD. Kinetic analysis of enzyme reactions. I. Further considerations of enzyme inhibition and analysis of enzyme activation. *Enzymologia* 15: 187–198, 1952.

Shapiro M & Brumer P. *Principles of the Quantum Control of Molecular Processes*. Hoboken, NJ: Wiley, 2003.

Shi L, Potts M & Kennelly PJ. The serine, threonine, and/or tyrosine-specific protein kinases and protein phosphatases of prokaryotic organisms: a family portrait. *FEMS Microbiol Rev* 22: 229–253, 1998.

Shimada A, Niwa H, Tsujita K, Suetsugu S, Nitta K, Hanawa-Suetsugu K, Akasaka R, Nishino Y, Toyama M, Chen L, Liu ZJ, Wang B, Yamamoto M, Terada T, Miyazawa A, Tanaka A, Sugano S, Shirouzu M, Nagayama K, Takenawa T & Yokoyama S. Curved EFC/F-BAR-domain dimers are joined end to end into a filament for membrane invagination in endocytosis. *Cell* 129: 761–772, 2007.

Shou M. Prediction of pharmacokinetics and drug–drug interactions from in vitro metabolism data. *Curr Opin Drug Discov Dev* 8: 66–77, 2005.

Sibley DR, Strasser RH, Benovic JL, Daniel K & Lefkowitz RJ. Phosphorylation/dephosphorylation of the beta-adrenergic receptor regulates its functional coupling to adenylate cyclase and subcellular distribution. *Proc Natl Acad Sci USA* 83: 9408–9412, 1986.

Silver RA, Colquhoun D, Cull-Candy SG & Edmonds B. Deactivation and desensitization of non-NMDA receptors in patches and the time course of EPSCs in rat cerebellar granule cells. *J Physiol* 493, 1996. Erratum in: *J Physiol* 496: 891: 167–173, 1996.

Stephenson SL, Stempen H & Stephen H. *Myxomycetes: Handbook of Slime Moulds*. Portland: Timber Press, 2000.

Stjernfelt F. *Diagrammatology: an Investigation on the Borderlines of Phenomenology, Ontology, and Semiotics*, 1st ed. Dordrecht: Springer Verlag, 2007.

Swillens S, Waelbroeck M & Champeil P. Does a radiolabelled ligand bind to a homogenous population of non-interacting receptor sites? *Trend Pharmacol Sci* 16: 151–155, 1995.

Szabadi E. A model of two functionally antagonistic receptor populations activated by the same agonist. *J Theor Biol* 69: 101–112, 1977.

Szurmant H, Mohan MA, Imus PM & Hoch JA. YycH and YycI interact to regulate the essential YycFG two-component system in *Bacillus subtilis*. *J Bacteriol* 189: 3280–3289, 2007.

Thomas D, Karle CA & Kiehn J. The cardiac hERG/IKr potassium channel as pharmacological target: structure, function, regulation, and clinical applications. *Curr Pharm Des* 12: 2271–2283, 2006.

Tomlinson G & Hnatowich MR. Apparent competitive inhibition of radioligand binding to receptors: experimental and theoretical considerations in the analysis of equilibrium binding data. *J Recept Res* 8: 809–830, 1988.

Trist DG & Leff P. Quantification of H2-agonism by clonidine and dimaprit in an adenylate cyclase assay. *Agents Actions* 16: 222–226, 1985.

Tucek S & Proska J. Allosteric modulation of muscarinic acetylcholine receptors. *Trends Pharmacol Sci* 16: 205–212, 1995.

Tucek S, Michal P & Vlachova V. Modelling the consequences of receptor-G-protein promiscuity. *Trends Pharmacol Sci* 23:171–176, 2002.

Tucek S, Musilkova J, Nedoma J, Proska J, Shelkovnikov S & Vorlicek J. Positive cooperativity in the binding of alcuronium and N-methylscopolamine to muscarinic acetylcholine receptors. *Mol Pharmacol* 38: 674–680, 1990.

Turchin P. Complex population dynamics: A theoretical/empirical synthesis. Princeton: Princeton University Press, 2003.

Urbe S. Ubiquitin and endocytic protein sorting. *Essays Biochem* 41: 81–98, 2005.

Urso B, Ilondo MM, Holst PA, Christoffersen CT, Ouwens M, Giorgetti S, Van Obberghen E, Naor D, Tornqvist H & De Meyts P. IRS-4 mediated mitogenic signalling by insulin and growth hormone in LB cells, a murine T-cell lymphoma devoid of IGF-I receptors. *Cell Signal* 15: 385–394, 2003.

Vauquelin G & Szczuka A. Kinetic versus allosteric mechanisms to explain insurmountable antagonism and delayed ligand dissociation. *Neurochem Int* 51: 254–260, 2007.

Vialou V, Balasse L, Dumas S, Giros B & Gautron S. Neurochemical characterization of pathways expressing plasma membrane monoamine transporter in the rat brain. *Neuroscience* 144: 616–622, 2007.

Vidler A. What is a diagram anyway? In: *Peter Eisenman: Feints*, 1st ed, edited by Cassara S. Milan: Skira, 2006.

Vieira OV, Verkade P, Manninen A, Simons K. FAPP2 is involved in the transport of apical cargo in polarized MDCK cells. *J Cell Biol* 170: 521–526, 2005.

Violin JD & Lefkowitz RJ. Beta-arrestin-biased ligands at seven-transmembrane receptors. *Trends Pharmacol Sci* 28: 416–422, 2007.

Volk T. *Gaia's Body. Toward a Physiology of Earth*, 1st ed. New York: Copernicus/Springer Verlag, 1997.

Waelbroeck M, Robberecht P, De Neef P & Christophe J. Effects of D-tubocurarine on rat cardiac muscarinic receptors: a comparison with gallamine. *J Recept Res* 8: 787–808, 1988.

Weiss ER, Raman D, Shirakawa S, Ducceschi MH, Bertram PT, Wong F, Kraft TW & Osawa S. The cloning of GRK7, a candidate cone opsin kinase, from cone- and rod-dominant mammalian retinas. *Mol Vis* 4: 27, 1998.

Wenz K. Representation and self-reference: Peirce's sign and its application to the computer. *Semiotica* 143: 199–209, 2003.

Wickramasinghe C. *A Journey with Fred Hoyle: the Search for Cosmic Life*. Singapore: World Scientific Publishing Co. Pte. Ltd., 2005.

Wickramasinghe NC. Fred Hoyle's Universe. Proceedings of a Conference celebrating Fred Hoyle's Extraordinary Contribution to Science, 25–26 June 2002. Cardiff: Cardiff University, 2003.

Winding B & Bindslev N. Desensitization and reactivation of ACh-regulated exocrine secretion in hen tracheal epithelium. *Am J Physiol* 264: C342–C351, 1993.

Wood D. *Time After Time*, 1st ed. Bloomington, IN: Indiana University Press, 2007.

Wreggett KA & Wells JW. Cooperativity manifest in the binding properties of purified cardiac muscarinic receptors. *J Biol Chem* 270: 22488–22499, 1995.

Wright EM, Hirayama BA & Loo DF. Active sugar transport in health and disease. *J Intern Med* 261: 32–43, 2007.

Zagotta WN, Hoshi T & Aldrich RW. Restoration of inactivation in mutants of Shaker potassium channels by a peptide derived from ShB. *Science* 250: 568–571, 1990.

Zhang J, Barak LS, Anborgh PH, Laporte SA, Caron MG & Ferguson SS. Cellular trafficking of G protein-coupled receptor/beta-arrestin endocytic complexes. *J Biol Chem* 274: 10999–21006, 1999.

Zhang M, Houamed K, Kupershmidt S, Roden D & Satin LS. Pharmacological properties and functional role of Kslow current in mouse pancreatic beta-cells: SK channels contribute to Kslow tail current and modulate insulin secretion. *J Gen Physiol* 126: 353–363, 2005.

Zhou J, Livak MF, Bernier M, Muller DC, Carlson OD, Elahi D, Maudsley S & Egan JM. Ubiquitination is involved in glucose-mediated downregulation of GIP receptors in islets. *Am J Physiol Endocrinol Metab* 293: E538–E547, 2007.

Zohar D, Marshall IN. *The Quantum Self*, 1st ed. London: Bloomsbury Publishing Plc, 1990.

Zwart R, Vijverberg HP. Potentiation and inhibition of neuronal alpha4beta4 nicotinic acetylcholine receptors by choline. *Eur J Pharmacol* 393: 209–214, 2000.